Energy, Mines and Resources Canada | Énergie, Mines et Ressources Canada

CANMET
Canada Centre for Mineral and Energy Technology | Centre canadien de la technologie des minéraux et de l'énergie

ANISOTROPIC PROPERTIES STUDY OF LAC DU BONNET GRANITE SPECIMENS: REPORT # 2

Rand Jackson
Rock Mechanics Laboratory

July 1986

This document is [illegible] report [illegible] (CANMET)

[illegible] rapport [illegible] et rédigé [illegible] de la technologie des minéraux et de l'énergie (CANMET)

MICROMEDIA

69 pp

MINERAL AND ENERGY TECHNOLOGY
MINING RESEARCH LABORATORIES
DIVISION REPORT M&ET/MRL 86-79(TR)

CONTENTS

		Page
1.	INTRODUCTION	1
2.	IDENTIFICATION OF SPECIMENS AND TESTS	1
3.	DESCRIPTION OF TEST MEASUREMENTS	3
4.	DATA TREATMENT	4
5.	DATA SUMMARY	5
6.	FAILURE CHARACTERISTICS	5
7.	ACKNOWLEDGEMENTS	5
8.	REFERENCES	6
	APPENDIX A	12

TABLES

No.		
1.	Summary of sample depth, dimensions, density and orientation	7
2.	Summary of ultrasonic velocity properties	9
3.	Summary of uniaxial compression properties	10

FIGURES

1.	Axial and circumferential stress/strain curves for anisotropy test specimens (Drill Hole 206-013-MOD1, Depth = 4.190 m)	30
2.	Axial and circumferential stress/strain curves for anisotropy test specimens (Drill Hole 206-013-MOD1, Depth = 4.282 m)	31
3.	Axial and circumferential stress/strain curves for anisotropy test specimens (Drill Hole 206-013-MOD1, Depth = 4.420 m)	32
4.	Axial and circumferential stress/strain curves for anisotropy test specimens (Drill Hole 206-013-MOD1, Depth = 4.657 m)	33
5.	Axial and circumferential stress/strain curves for anisotropy test specimens (Drill Hole 206-013-MOD1, Depth = 4.756 m)	34
6.	Axial and circumferential stress/strain curves for anisotropy test specimens (Drill Hole 206-013-MOD1, Depth = 4.892 m)	35
7.	Axial and circumferential stress/strain curves for anisotropy test specimens (Drill Hole 206-013-MOD1, Depth = 4.947 m)	36
8.	Axial and circumferential stress/strain curves for anisotropy test specimens (Drill Hole 206-013-MOD1, Depth = 5.002 m)	37

FIGURES (Cont'd)

No.		Page
9.	Axial and circumferential stress/strain curves for anisotropy test specimens (Drill Hole 206-013-MOD1, Depth = 5.062 m)	38
10.	Axial and circumferential stress/strain curves for anisotropy test specimens (Drill Hole 206-016-MOD1, Depth = 5.252 m)	39
11.	Axial and circumferential stress/strain curves for anisotropy test specimens (Drill Hole 206-016-MOD1, Depth = 5.342 m)	40
12.	Axial and circumferential stress/strain curves for anisotropy test specimens (Drill Hole 206-016-MOD1, Depth = 5.482 m)	41
13.	Axial and circumferential stress/strain curves for anisotropy test specimens (Drill Hole 206-016-MOD1, Depth = 5.717 m)	42
14.	Axial and circumferential stress/strain curves for anisotropy test specimens (Drill Hole 206-016-MOD1, Depth = 5.817 m)	43
15.	Axial and circumferential stress/strain curves for anisotropy test specimens (Drill Hole 206-016-MOD1, Depth = 5.952 m)	44
16.	Axial and circumferential stress/strain curves for anisotropy test specimens (Drill Hole 206-016-MOD1, Depth = 6.002 m)	45
17.	Axial and circumferential stress/strain curves for anisotropy test specimens (Drill Hole 206-016-MOD1, Depth = 6.052 m)	46
18.	Axial and circumferential stress/strain curves for anisotropy test specimens (Drill Hole 206-016-MOD1, Depth = 6.102 m)	47
19.	Axial and circumferential stress/strain curves for anisotropy test specimens (Drill Hole 001-041-MOD1, Depth = 2.060 m)	48
20.	Axial and circumferential stress/strain curves for anisotropy test specimens (Drill Hole 001-041-MOD1, Depth = 2.152 m)	49
21.	Axial and circumferential stress/strain curves for anisotropy test specimens (Drill Hole 001-041-MOD1, Depth = 2.290 m)	50
22.	Axial and circumferential stress/strain curves for anisotropy test specimens (Drill Hole 001-041-MOD1, Depth = 2.527 m)	51
23.	Axial and circumferential stress/strain curves for anisotropy test specimens (Drill Hole 001-041-MOD1, Depth = 2.626 m)	52
24.	Axial and circumferential stress/strain curves for anisotropy test specimens (Drill Hole 001-041-MOD1, Depth = 2.751 m)	53
25.	Axial and circumferential stress/strain curves for anisotropy test specimens (Drill Hole 001-141-MOD1, Depth = 2.808 m)	54

FIGURES (Cont'd)

No.		Page
26.	Axial and circumferential stress/strain curves for anisotropy test specimens (Drill Hole 001-041-MOD1, Depth = 2.862 m)	55
27.	Axial and circumferential stress/strain curves for anisotropy test specimens (Drill Hole 001-041-MOD1, Depth = 2.917 m)	56
28.	Axial and circumferential stress/strain curves for anisotropy test specimens (Drill Hole 001-041-MOD2, Depth = 2.475 m)	57
29.	Axial and circumferential stress/strain curves for anisotropy test specimens (Drill Hole 001-041-MOD2, Depth = 2.565 m)	58
30.	Axial and circumferential stress/strain curves for anisotropy test specimens (Drill Hole 001-041-MOD2, Depth = 2.705 m)	59
31.	Axial and circumferential stress/strain curves for anisotropy test specimens (Drill Hole 001-041-MOD2, Depth = 2.938 m)	60
32.	Axial and circumferential stress/strain curves for anisotropy test specimens (Drill Hole 001-041-MOD2, Depth = 3.038 m)	61
33.	Axial and circumferential stress/strain curves for anisotropy test specimens (Drill Hole 001-041-MOD2, Depth = 3.170 m)	62
34.	Axial and circumferential stress/strain curves for anisotropy test specimens (Drill Hole 001-041-MOD2, Depth = 3.220 m)	63
35.	Axial and circumferential stress/strain curves for anisotropy test specimens (Drill Hole 001-041-MOD2, Depth = 3.270 m)	64
36.	Axial and circumferential stress/strain curves for anisotropy test specimens (Drill Hole 001-041-MOD2, Depth = 3.320 m)	65

1. INTRODUCTION

As part of the Canadian Nuclear Fuel Waste Management Project (NFWMP), Atomic Energy of Canada Limited (AECL) is characterizing various rock formations to determine their suitability for long term disposal of high level wastes. The program also includes the construction of an underground research laboratory (URL) near Pinawa, Manitoba to provide an opportunity for extensive in situ investigations.

Biaxial testing conducted on core obtained during the construction phase of the URL has indicated that the rock may be anisotropic in terms of modulus of elasticity (1). It was felt that further study in the form of acoustic velocity and uniaxial compression testing could provide additional insight into this behaviour. The program is currently ongoing and will continue as new samples are obtained from the URL site.

This report represents the second of a series of reports which will be published as new data becomes available. No attempt will be made to analyze the data until the program is completed.

2. IDENTIFICATION OF SPECIMENS AND TESTS

Thirty six samples were used for this test series: 9 from each of drill holes 206-013-MOD1, 206-016-MOD1, 001-041-MOD1 and 001-041-MOD2. The location and orientation of the drill holes can be found in Appendix A and are summarized below:

206-013-MOD1:	Collar Coordinates:	N 5,570,459.138
		E 295,801.045
		elev. 52.674
	Orientation:	Plunge (dip): -00.86° (up)
		Trend (direction): 020.97°
206-016-MOD1:	Collar Coordinates:	N 5,570,457.186
		E 295,802.432
		elev. 53.255
	Orientation:	Plunge (dip): -02.99° (up)
		Trend (direction): 113.95°

001-041-MOD1:	Collar Coordinates:	N 5,570,476.120
		E 295,787.639
		elev. 41.089
	Orientation:	Plunge (dip): -02.68° (up)
		Trend (direction): 069.09°
001-041-MOD2:	Collar Coordinates:	N 5.570,473.642
		E 295,785.900
		elev. 40.637
	Orientation:	Plunge (dip): -01.70° (up)
		Trend (direction): 157.78°

The 45 mm test specimens were prepared by recoring the 200 mm cores obtained from the drill holes along the axes of interest. The specimens were then identified according to their location and orientation as follows:

a) depth of the collar of the 45 mm hole from the collar of the 200 mm hole;
b) angle β gives the location of the collar of the 45 mm hole around the circumference of the 200 mm core. The angle is measured clockwise (looking down hole) from the orientation mark on the top of the core;
c) angle α is the angle between the core axis of the 45 mm core and the 200 mm core. The angle is measured clockwise (i.e., dip) from the down hole direction of the 200 mm core.

Table 1 provides a summary of the specimen depth, dimensions, density and orientation. The following properties were determined for the samples listed:

1. compressive wave velocity;
2. shear wave velocity;
3. dynamic shear modulus, G_d;
4. dynamic Young's modulus, E_d;
5. Poisson's ratio (determined using velocity data), V_d;
6. uniaxial compressive strength;
7. Poisson's ratio, ν;
8. tangent modulus of elasticity, E_t; and
9. secant modulus of elasticity, E_s.

Dynamic constants were unavailable for samples obtained from boreholes 206-016-MOD1 and 001-041-MOD1 due to equipment failure during testing.

3. DESCRIPTION OF TEST MEASUREMENTS

Compression and shear wave velocity measurements were carried out on samples already gauged for elastic deformation measurement. The testing equipment consisted of: transmitting and receiving platens containing piezoelectric transducers, a high voltage pulse generator, a signal amplifier and a Tektronix Type 555 dual beam oscilloscope equipped with delay sweep and a time base resolution of 0.01 micro-seconds. The zero time delay was determined by measuring the time of wave arrival across three steel samples of different lengths. These arrival times could then be extrapolated to correspond to a specimen of zero length.

For an outline of the uniaxial compression procedure, the reader is referred to Technical Data 303410-M01/78 (2). The two Phillips PR 9302 strain bridges and the Mosely Autograph 2FRA X-Y recorder referred to in that document were replaced, in the present study, by two Bruel and Kjaer Type 1526 strain indicators and a Hewlett Packard 7046B X-Y recorder. These equipment were used to measure and record the axial and transverse strains as a function of axial load. Linear variable differential transducers (LVDT's) were also utilized to provide redundant measurements of axial deformation.

4. DATA TREATMENT

The compressional and shear wave velocities were determined by dividing the specimen length by the wave travel time through the specimen. The dynamic properties were, then, calculated using the following equations (3):

Dynamic Shear Modulus

$$G_d = \rho V_s^2 \qquad \text{Eq 1}$$

where: G = dynamic shear modulus
V = shear wave velocity
ρ = density

Dynamic Young's Modulus

$$E_d = \frac{\rho V_s^2 (3V_p^2 - 4V_s^2)}{V_p^2 - V_s^2} \qquad \text{Eq 2}$$

where: E_d = dynamic Young's modulus
V_s = shear wave velocity
V_p = compressional wave velocity
ρ = density

Poisson's Ratio (based on velocity data)

$$V_d = \frac{V_p^2 - 2V_s^2}{2(V_p^2 - V_s^2)} \qquad \text{Eq 3}$$

where: V_d = Poisson's ratio
V_s = shear wave velocity
V_p = compressional wave velocity

The tangent modulus of elasticity (E_t) was calculated for each sample by determining the slope of the tangent to the axial strain curve at 50% of the failure load. The secant modulus of elasticity (E_s) was calculated by determining the slope of the line joining the origin to the point on the axial strain curve corresponding to 50% of the failure load. The ultimate compressive strength of each sample was calculated by dividing the sample failure load by the sample's cross-sectional area. The ratio of the tangent to the transverse strain curve to the tangent to the axial strain curve, at 50% failure load, was used to determine the sample Poisson's ratio (ν).

5. DATA SUMMARY

Table 2 contains the results of the ultrasonic velocity measurements including the calculated values of the dynamic shear modulus, dynamic Young's modulus as well as Poisson's ratio estimated on the basis of velocity data for each sample. Table 3 summarizes the uniaxial compression measurements which include determinations of the loading rate, uniaxial compressive strength, tangent modulus of elasticity, secant modulus of elasticity, Poisson's ratio and the predominant mode of failure for each specimen.

Figures 1 through 36 represent the circumferential and axial stress/strain curves for each sample. Also included on the figures is a summary of the sample's depth, orientation, tangent modulus and Poisson's ratio.

6. FAILURE CHARACTERISTICS

The predominant mode of failure was that of a double wedge or double cone configuration. These were accompanied by considerable axial splitting and slabbing. Partially formed single diagonal failure planes were apparent in several samples although the explosive nature of the failures made it impossible to measure the angles.

7. ACKNOWLEDGEMENTS

The author would like to acknowledge the valuable assistance of Ms. Sylvie Ratte during this test program.

8. REFERENCES

1. Lang, P. Personal communication; 1985.

2. Annor, A. and Geller, L. "Dilatational velocity, Young's modulus, Poisson's ratio, uniaxial compressive strength and Brazilian tensile strength for WN1 and WN2 samples"; CANMET/MRL Technical Data 303410-M01/78; 1978.

3. Lama, R.D., Saluja, S.S. and Vutikuri, V.S. "Handbook on mechanical properties of rocks"; Volume II, Chapter 7; Trans Tech Publications.

Table 1 - Summary of sample depth, dimensions, density and orientation

Drill hole	Sample depth (m)	Length (mm)	Diameter (mm)	Density (g/cm^3)	Orientation α	Orientation β
206-013-MOD1	4.190	111.40	44.44	2.64	0°	-
	4.282	111.83	44.50	2.63	30°	0°
	4.420	110.02	44.43	2.64	30°	90°
	4.657	111.07	44.42	2.64	60°	0°
	4.756	102.03	44.42	2.89	60°	90°
	4.892	112.46	44.46	2.64	90°	0°
	4.947	110.38	44.49	2.64	90°	30°
	5.002	110.49	44.44	2.65	90°	60°
	5.062	111.09	44.50	2.64	90°	90°
206-016-MOD1	5.252	112.36	44.52	2.64	0°	-
	5.342	111.12	44.52	2.66	30°	0°
	5.482	110.43	44.48	2.63	60°	0°
	5.717	112.22	44.48	2.64	60°	90°
	5.817	111.98	44.48	2.65	90°	0°
	5.952	113.60	44.52	2.66	90°	30°
	6.002	109.14	44.52	2.67	90°	60°
	6.052	109.19	44.48	2.68	90°	60°
	6.102	109.51	44.48	2.67	90°	90°
001-041-MOD1	2.060	105.14	44.48	2.63	0°	-
	2.152	99.76	44.32	2.62	30°	0°
	2.290	105.00	44.36	2.62	30°	90°
	2.527	110.79	44.44	2.62	60°	0°
	2.626	108.52	44.44	2.64	60°	90°
	2.751	109.97	44.50	2.63	90°	0°
	2.808	110.66	44.50	2.62	90°	30°
	2.862	110.10	44.50	2.62	90°	60°
	2.917	107.29	44.50	2.63	90°	90°

Table 1 (Cont'd)

Drill hole	Sample depth (m)	Length (mm)	Diameter (mm)	Density (g/cm^3)	Orientation α	Orientation β
001-041-MOD2	2.475	106.35	44.46	2.64	0°	-
	2.565	112.96	44.48	2.63	30°	0°
	2.705	108.27	44.49	2.63	30°	90°
	2.938	111.87	44.44	2.63	60°	0°
	3.038	108.37	44.43	2.64	60°	90°
	3.170	108.24	44.44	2.63	90°	0°
	3.220	112.95	44.42	2.62	90°	30°
	3.270	101.05	44.50	2.89	90°	60°
	3.320	110.29	44.47	2.63	90°	90°

Table 2 - Summary of ultrasonic velocity properties

Drill hole	Sample depth (m)	P-wave velocity (km/s)	S-wave velocity (km/s)	Dynamic shear modulus, G (GPa)	Dynamic Young's modulus, E_d (GPa)	Dynamic Poisson's ratio
206-013-MOD1	4.190	4.39	3.20	27.03	50.45	-0.07
	4.282	4.52	3.31	28.81	53.12	-0.08
	4.420	4.02	2.97	23.29	41.87	-0.10
	4.657	4.79	3.39	30.34	60.57	-0.02
	4.756	3.46	2.65	20.30	32.09	-0.21
	4.892	4.80	3.44	31.24	60.73	-0.03
	4.947	4.83	3.47	31.79	61.46	-0.03
	5.002	4.40	3.24	27.82	50.50	-0.09
	5.062	3.94	2.99	23.60	38.76	-0.18
001-041-MOD2	2.475	3.98	2.84	21.29	41.79	-0.02
	2.565	4.19	3.19	26.76	43.39	-0.19
	2.705	4.22	2.74	19.74	44.84	0.14
	2.938	4.72	3.40	30.40	58.42	-0.04
	3.038	4.63	2.93	22.66	52.85	0.17
	3.170	4.92	3.40	30.40	63.42	0.04
	3.220	4.68	3.37	29.76	57.22	-0.04
	3.270	3.89	2.86	23.64	43.11	-0.09
	3.320	4.12	3.03	24.15	43.99	-0.09

Table 3 - Summary of uniaxial compression properties

Drill hole	Sample depth (m)	Loading rate (MPa/s)	Uniaxial compressive strength (MPa)	Tangent modulus of elasticity (GPa)	Second modulus of elasticity (GPa)	Poisson's ratio	Predominant failure characteristic
206-013-MOD1	4.190	1.07	186	62.22	48.71	0.24	diagonal failure plane
	4.282	1.04	177	66.55	49.54	0.38	diagonal failure plane
	4.420	1.11	208	68.50	48.46	0.29	double wedge
	4.657	1.39	203	71.57	58.78	0.26	double wedge
	4.756	1.15	210	65.71	45.15	0.24	bottom wedge
	4.892	1.17	191	63.16	54.74	0.28	double wedge
	4.947	1.14	191	65.76	54.89	0.26	diagonal failure plane
	6.002	1.21	197	63.86	46.88	0.28	diagonal failure plane
	5.062	1.06	221	67.10	48.58	0.24	double wedge
206-016-MOD1	5.252	1.23	215	74.23	51.25	0.28	double wedge
	5.342	1.16	199	70.55	52.22	0.24	bottom wedge
	5.482	0.82	172	69.87	48.87	0.27	diagonal failure plane
	5.717	1.09	197	63.68	49.52	0.22	double wedge
	5.817	0.79	172	74.49	52.02	0.30	top wedge
	5.952	1.18	216	70.29	65.09	0.22	bottom wedge
	6.002	1.13	242	68.21	60.38	0.21	diagonal failure plane
	6.052	1.17	247	69.17	58.86	0.27	double wedge
	6.102	0.86	164	61.04	48.69	0.25	diagonal failure plane
001-041-MOD1	2.060	1.16	201	65.96	44.49	0.30	double cone
	2.152	0.99	170	69.40	45.18	0.25	double wedge
	2.290	0.95	176	55.63	36.12	0.30	diagonal failure plane
	2.527	0.90	168	59.53	41.86	0.29	double wedge
	2.626	0.86	120	48.87	42.39	0.23	bottom wedge
	2.751	0.90	174	63.81	48.38	0.29	double wedge
	2.808	0.78	127	63.85	52.74	0.35	double wedge
	2.862	1.08	187	64.02	45.15	0.22	double wedge
	2.917	1.17	185	60.42	38.00	0.24	double wedge

Table 3 (Cont'd)

Drill hole	Sample depth (m)	Loading rate (MPa/s)	Uniaxial compressive strength (MPa)	Tangent modulus of elasticity (GPa)	Second modulus of elasticity (GPa)	Poisson's ratio	Predominant failure characteristic
001-041-MOD2	2.475	0.98	210	62.86	41.88	0.24	double cone
	2.565	1.15	205	66.60	49.61	0.23	diagonal failure plane
	2.705	0.77	219	68.38	46.91	0.24	double wedge
	2.938	0.89	191	69.09	55.93	0.28	diagonal failure plane
	3.038	1.15	235	70.10	50.46	0.22	double wedge
	3.170	0.96	182	66.62	56.72	0.25	diagonal failure plane
	3.220	0.94	205	69.48	56.26	0.25	diagonal failure plane
	3.270	1.00	208	66.01	48.98	0.26	double wedge
	3.320	1.11	209	64.36	48.11	0.24	double wedge

APPENDIX A

Atomic Energy of Canada Limited
Research Company
Whiteshell Nuclear Research Establishment

L'Énergie Atomique du Canada, Limitée
Société de Recherche
Etablissement de Recherches Nucléaires de Whiteshell

Pinawa
Manitoba
Canada
R0E 1L0
(204) 753-2311
Telex 07-57553
Twx 610-672-8141

1986 March 10 GSEB-86-042

Mr. Alfred Annor
CANMET
555 Booth Street
OTTAWA, Ontario
K1A 0G1

Dear Alfred:

The third batch of anisotropic properties samples will be sent to you this week. This batch consists of 36 samples from four 200 mm cores from drill hole numbers 206-016-MOD1, 206-013-MOD1, 001-041-MOD1, 001-041-MOD2.

The attachments give the details of the 200 mm drill hole locations, the system for describing the 45 mm core location and orientation, and photographs of the samples. The sampling method was described in the previous letter and attachments.

If you have any questions, please call be at (204) 345-8625.

Yours truly,

P. A. Lang
Geotechnical Science and
Engineering Branch

PLA/pyc

Attachments

cc: P. M. Thompson
G. R. Simmons
S. H. Whitaker
S. Daley

DESIGNATION OF ANISOTROPIC PROPERTIES SAMPLES

The location and orientation of the 200 mm diameter core hole numbers are as follows:

206-016-MOD1
Collar Coordinates : N 5,570,457.186
E 295,802.432
elev. 53.255
Orientation : Plunge (dip): -02.99° (up)
: Trend (direction): 113.95°

206-013-MOD1
Collar Coordinates : N 5,570,459.138
E 295,801.045
elev. 52.674
Orientation : Plunge (dip): -00.86° (up)
: Trend (direction): 020.97°

001-041-MOD1
Collar Coordinates : N 5,570,476.120
E 295,787.639
elev. 41.089
Orientation: : Plunge (dip): -02.68° (up)
: Trend (direction): 069.09°

001-041-MOD2
Collar Coordinates : N 5,570,473.642
E 295,785.900
elev. 40.637
Orientation : Plunge (dip): -01.70° (up)
: Trend (direction): 157.78

The location and orientation of the 45 mm cores taken from the 200 mm cores are defined as follows:

a) depth of the collar of the 45 mm hole from the collar of the 200 mm hole

b) angle β gives the location of the collar of the 45 mm hole around the circumference of the 200 mm core. The angle is measured clockwise (looking down hole) from the orientation mark on the top of the core.

c) angle α is the angle between the core axis of the 45 mm core and the 200 mm core. The angle is measured clockwise (i.e. dip) from the down hole direction of the 200 mm core.

The depth, and α and β angles are maked on each core, and on a label on water proof paper attached to each core. They are also listed in Tables 1 to 4.

- Attachment 1

In addition to these markings, there are two lines, an arrow, and β angle on the collar end of each 45 mm core (except the axial core). One line indicates the axial direction of the 200 mm core and the arrow points down hole. The short line across the axial line indicates the point at which the depth is measured. The 45 mm core that is parallel to the 200 mm core axis, contains the axial line and arrow marked along the top of the core. Pieces of core that are not suitable for testing are marked "DO NOT TEST".

Three pieces of core are not suitable for testing due to being partially drilled into while obtaining another sample. Redrilling was not necessary because other pieces of the samples were more than 110 mm in length. The above mentioned are marked "DO NOT TEST" and listed below:

206-013-MOD1
α 30° β 90°
Depth 4.420 m

001-041-MOD1
α 30° β 0°
Depth 2.152 m

001-041-MOD2
α 30° β 0°
Depth 2.565

Steve Daley

Steve Daley
1986 March 10

TABLE 1

DRILL HOLE NO. 206-016-MOD1
5.252 to 6.233
MARK TOP OF HOLE AND AXIAL DIRECTIONS

DEPTH (m)	α (From Axial)	β (Around Circumference)	DATE DRILLED
5.252	0°	Axial Core	86-01-27
5.342	30°	0°	86-01-31
5.482	30°	90°	86-01-31
5.717	60°	0°	86-01-31
5.817	60°	90°	86-01-31
5.952	90°	0°	86-01-28
6.002	90°	30°	86-01-28
6.052	90°	60°	86-01-28
6.102	90°	90°	86-01-28

TABLE 2

DRILL HOLE NO. 206-013-MOD1
4.190 to 5.115
MARK TOP OF HOLE AND AXIAL DIRECTIONS

DEPTH (m)	α (From Axial)	β (Around Circumference)	DATE DRILLED
4.190	0°	Axial Core	86-01-27
4.282	30°	0°	86-01-29
4.420	30°	90°	86-01-29
4.657	60°	0°	86-01-29
4.756	60°	90°	86-01-29
4.892	90°	0°	86-01-28
4.947	90°	30°	86-01-28
5.002	90°	60°	86-01-28
5.062	90°	90°	86-01-28

TABLE 3

DRILL HOLE NO. 001-041-MOD1
2.060 to 2.950
MARK TOP OF HOLE AND AXIAL DIRECTIONS

DEPTH (m)	α (From Axial)	β (Around Circumference)	DATE DRILLED
2.060	0°	AXIAL CORE	86-01-27
2.152	30°	0°	86-01-30
2.290	30°	90°	86-01-30
2.527	60°	0°	86-01-30
2.626	60°	90°	86-01-30
2.751	90°	0°	86-01-28
2.808	90°	30°	86-01-28
2.862	90°	60°	86-01-28
2.917	90°	90°	86-01-28

TABLE 4

DRILL HOLE NO. 001-041-MOD2
2.475 TO 3.380
MARK TOP OF HOLE AND AXIAL DIRECTIONS

DEPTH (m)	α (From Axial)	β (Around Circumference)	DATE DRILLED
2.475	0°	Axial Core	86-01-27
2.565	30°	0°	86-01-31
2.705	30°	90°	86-01-30
2.938	60°	0°	86-01-30
3.038	60°	90°	86-01-30
3.170	90°	0°	86-01-28
3.220	90°	30°	86-01-28
3.270	90°	60°	86-01-28
3.320	90°	90°	86-01-28

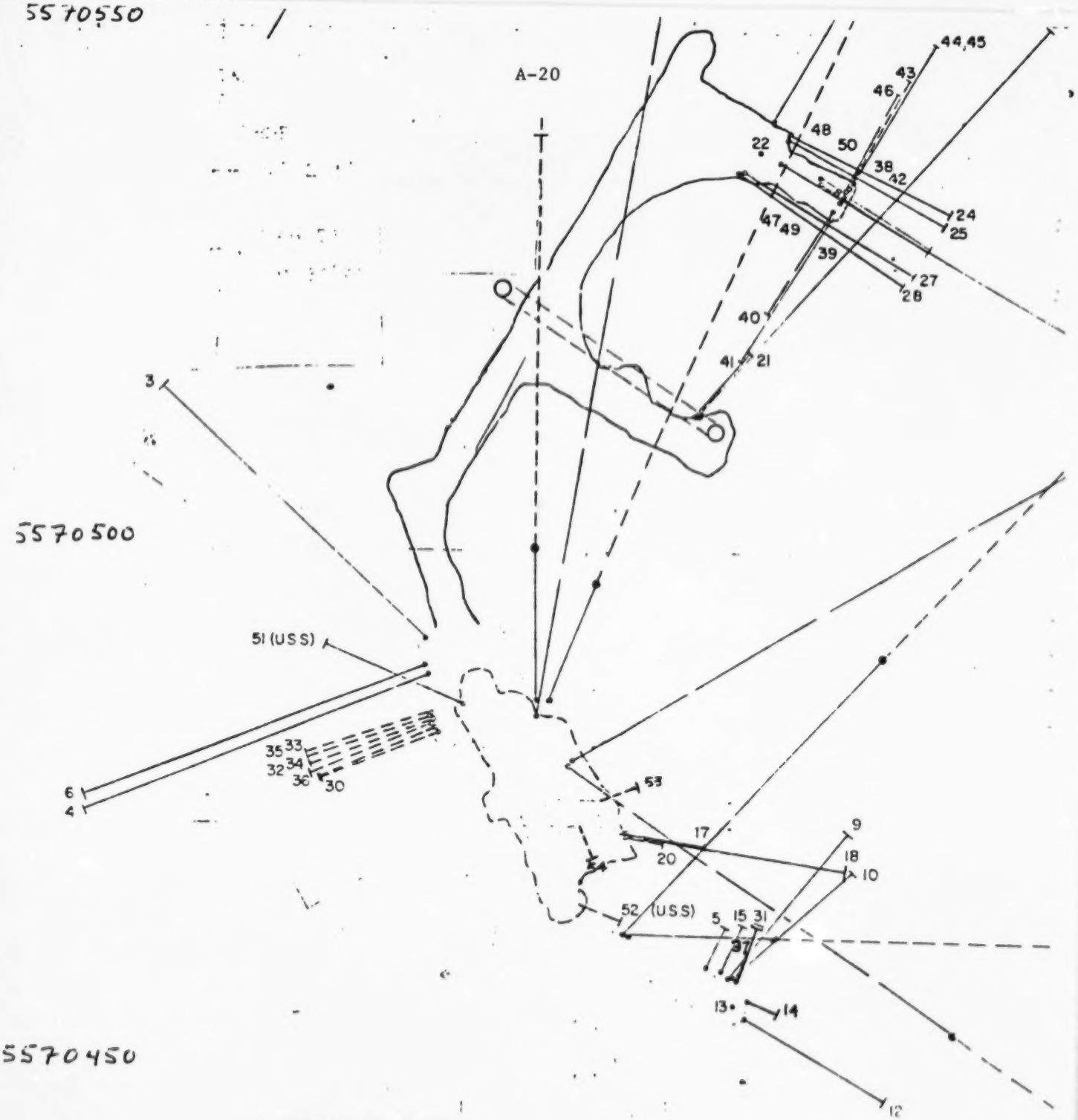

14 206-016-MOD1
37 206-013-MOD1
53 001-041-MOD1
54 001-041-MOD2

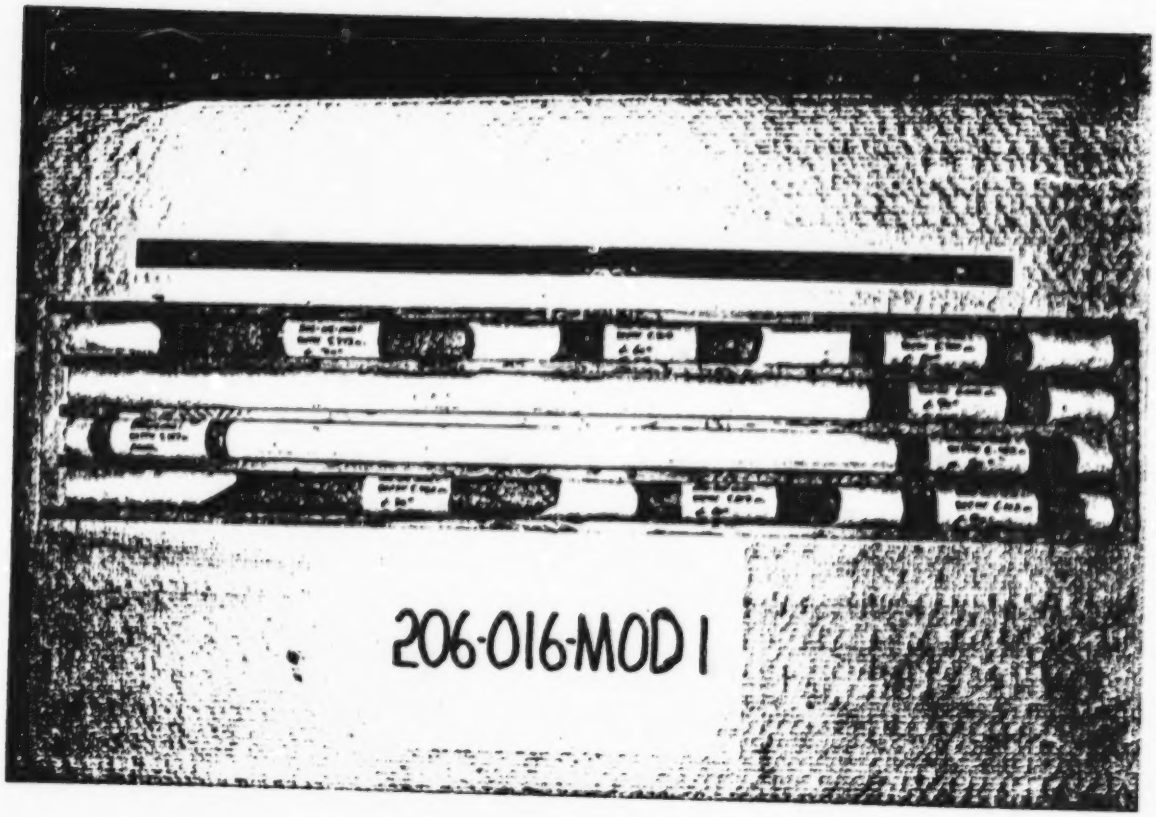
206-016-MOD 1

206-016-MOD 1

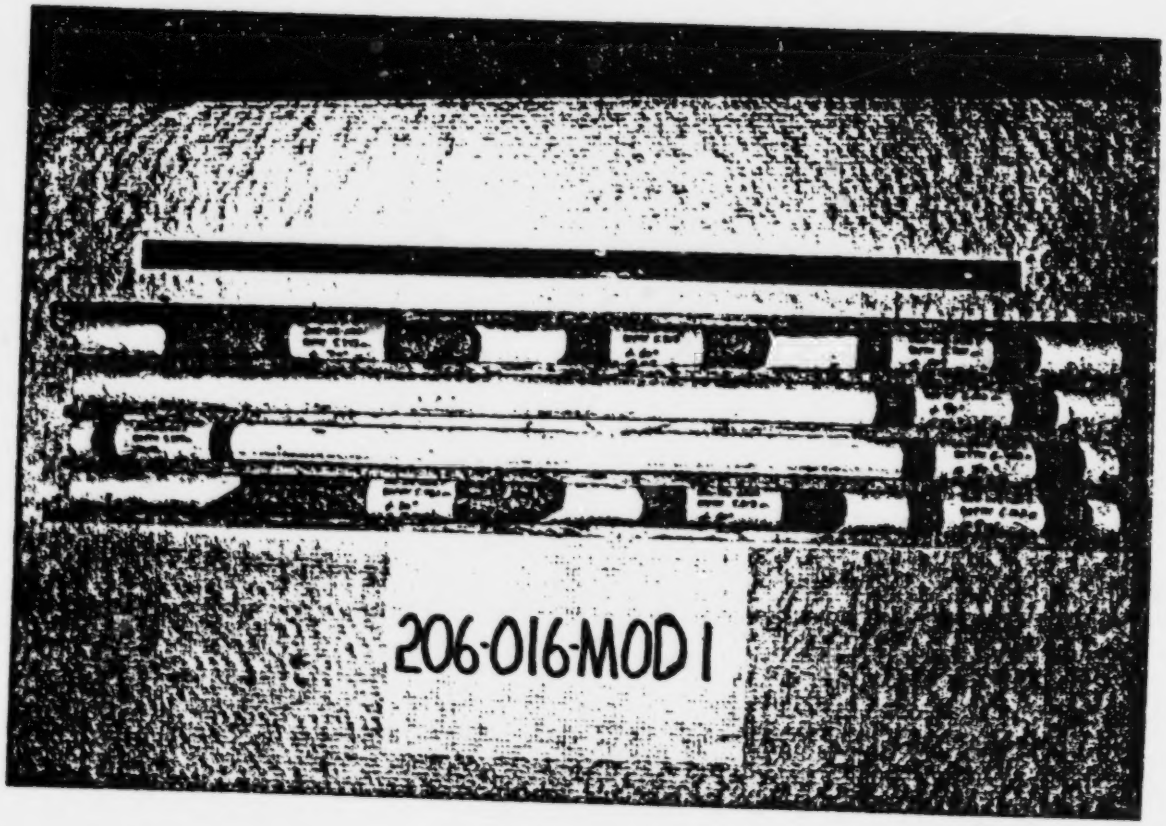
206-016-MOD 1

206-016-MOD 1

206-016-MOD 1

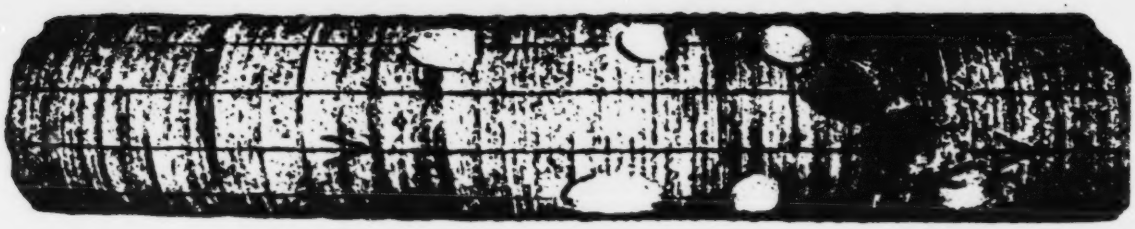

206-016-MOD 1

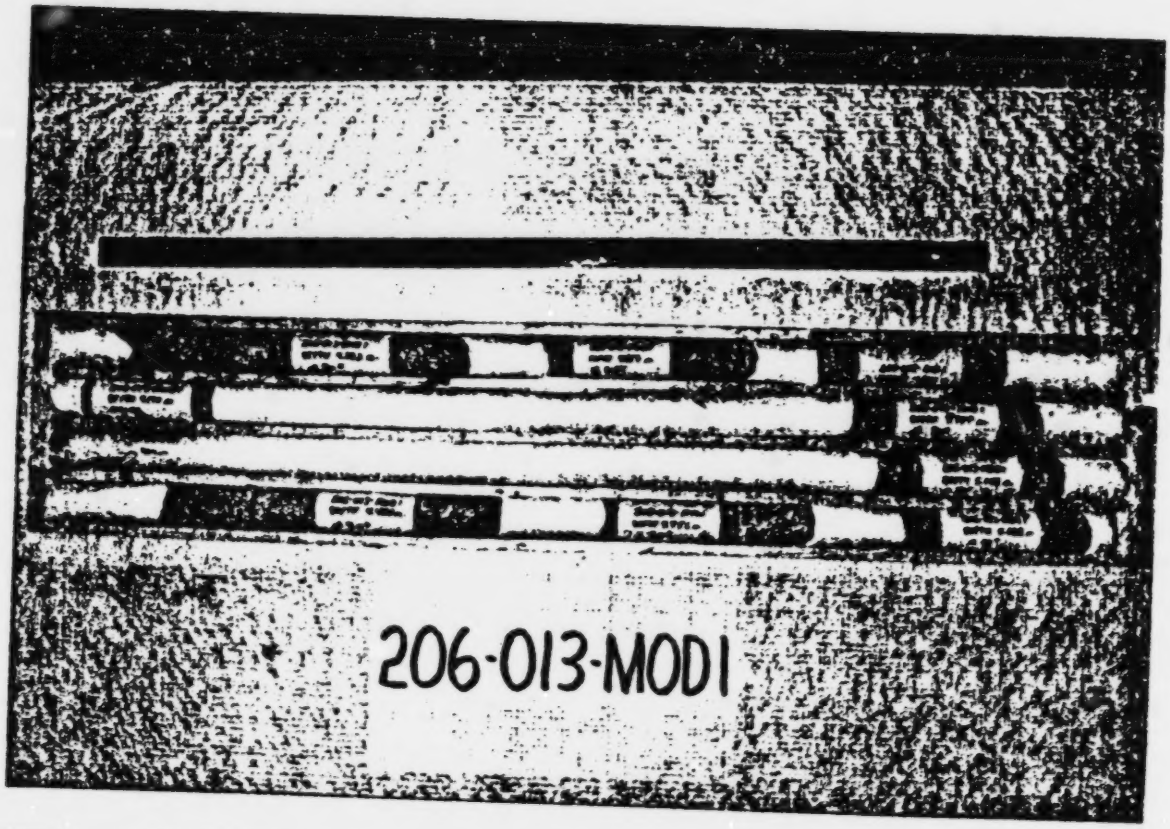
206-013-MOD1

206-013-MOD1

[redacted]

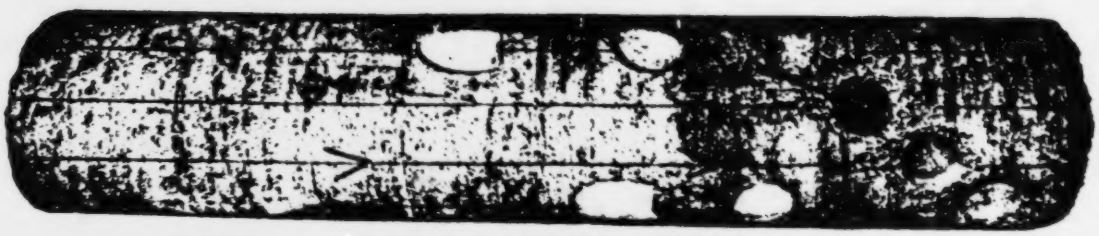

206-013-MOD1

[redacted]

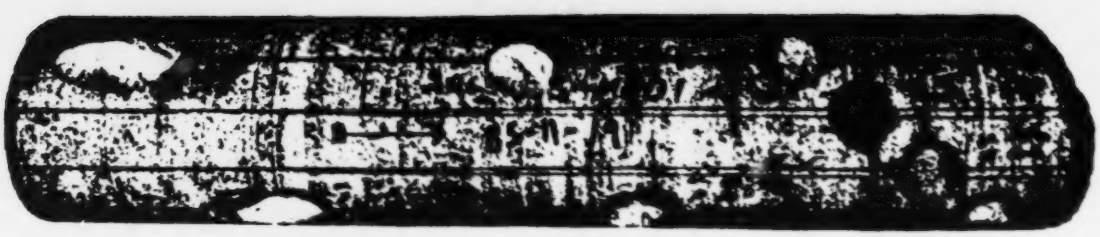

206-013-MOD1

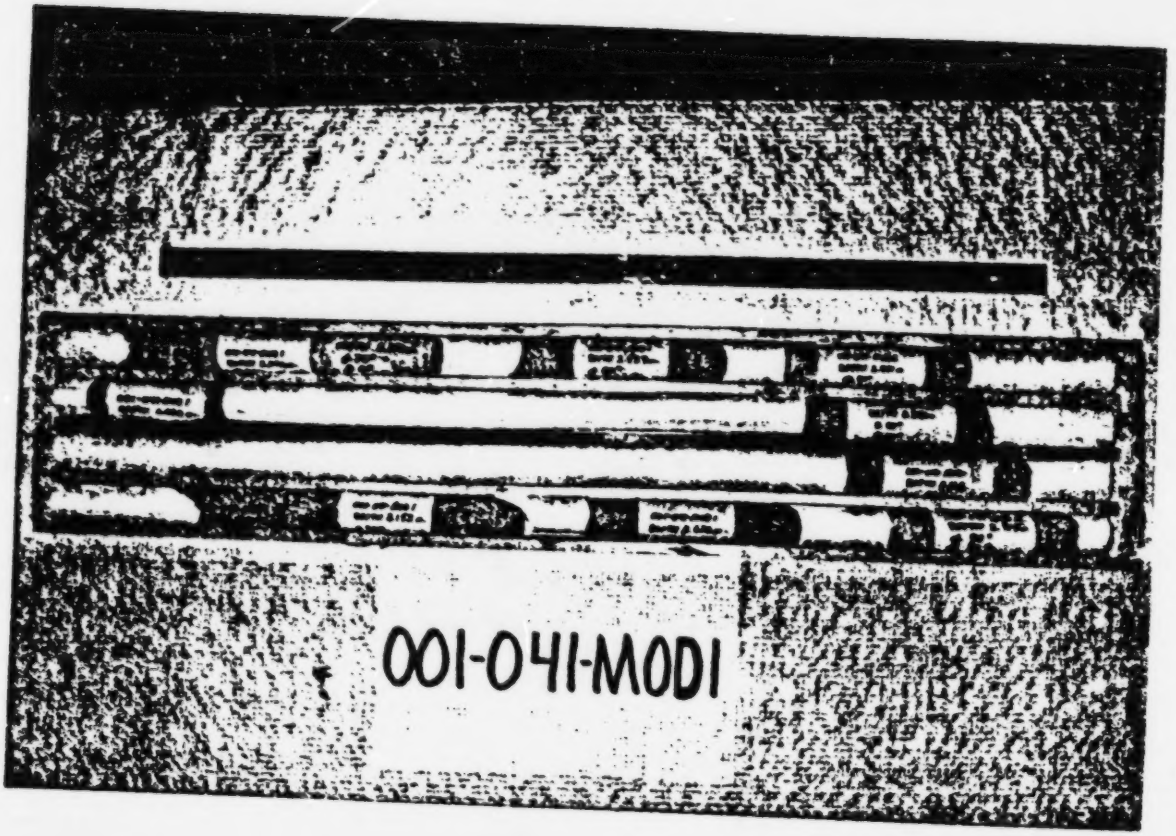
001-041-MOD1

001-041-MOD1

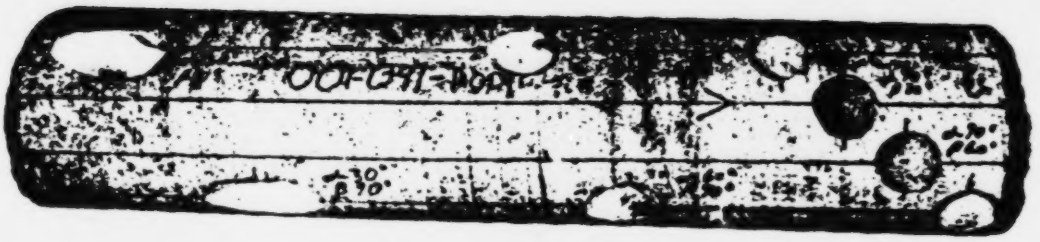

001-041-MOD1

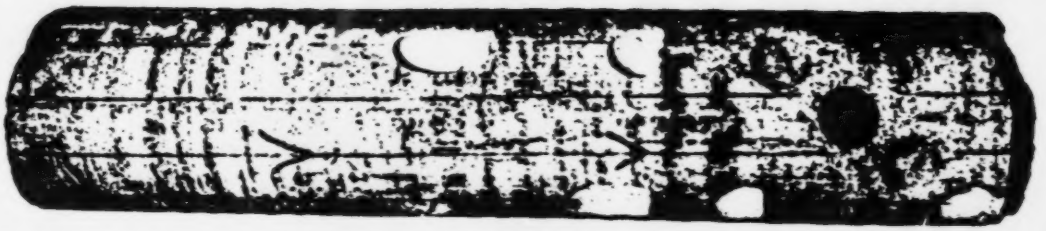

001-041-MOD1

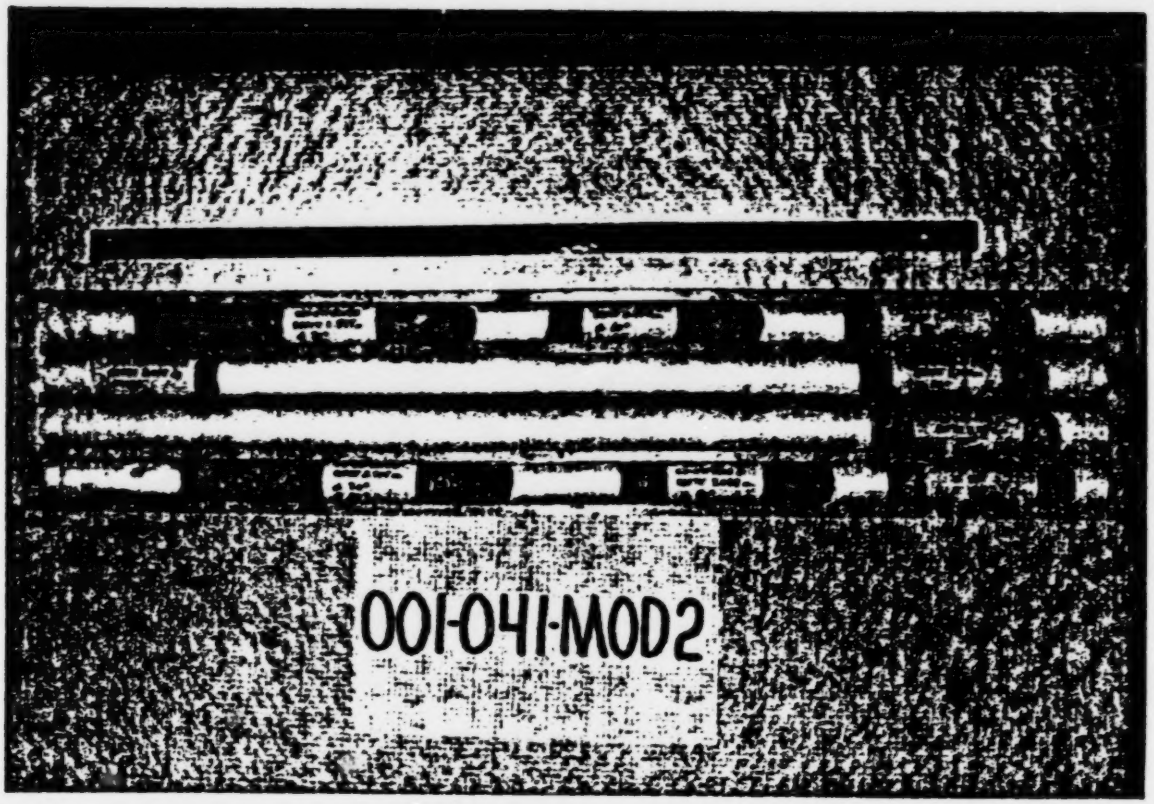
001-041-MOD2

001-041-MOD2

[redacted]

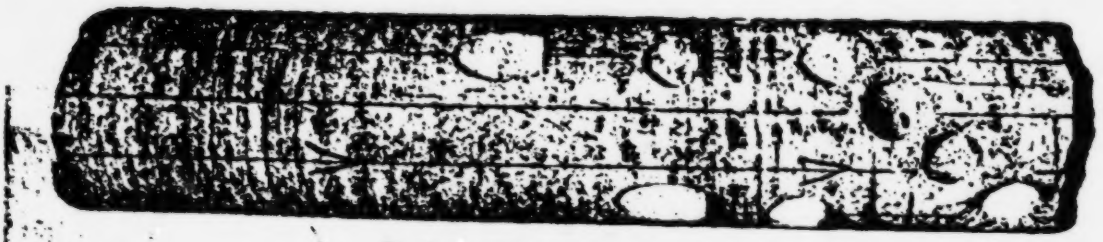

001-041-MOD2

[redacted]

001-041-MOD2

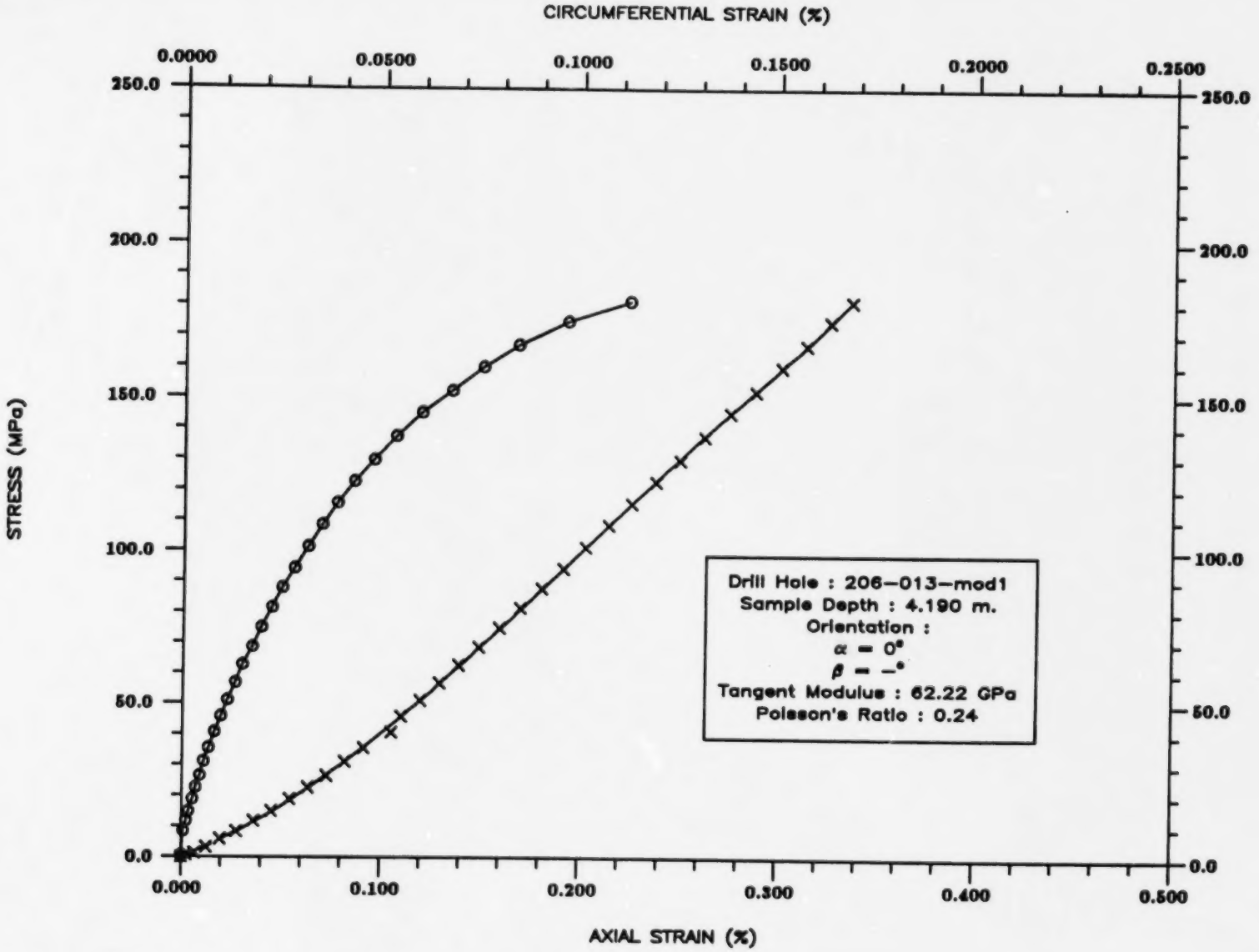

Fig. 1 : Axial and circumferential stress/strain curves for anisotropy test specimens.

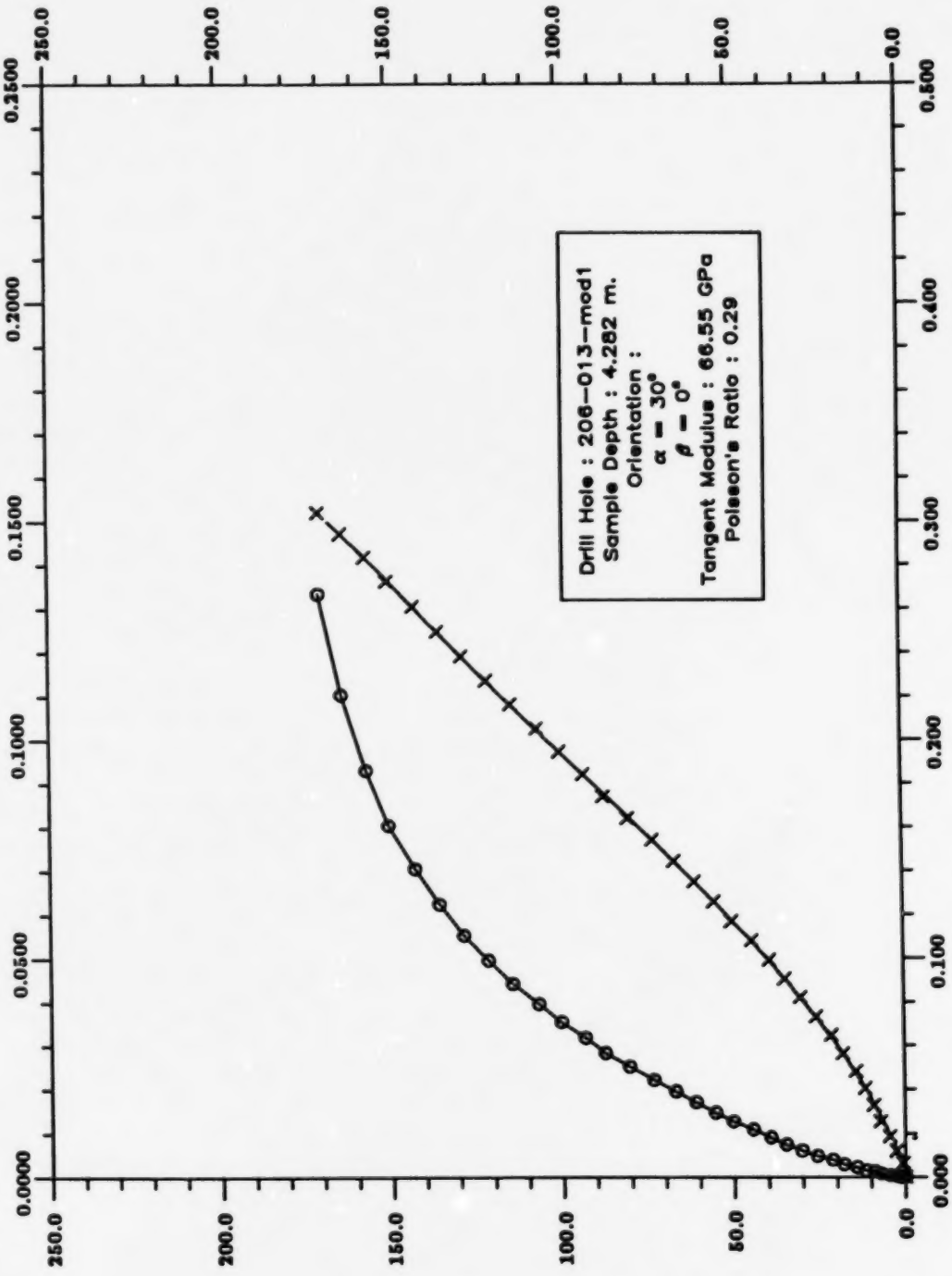

Fig. 2 : Axial and circumferential stress/strain curves for anisotropy test specimens.

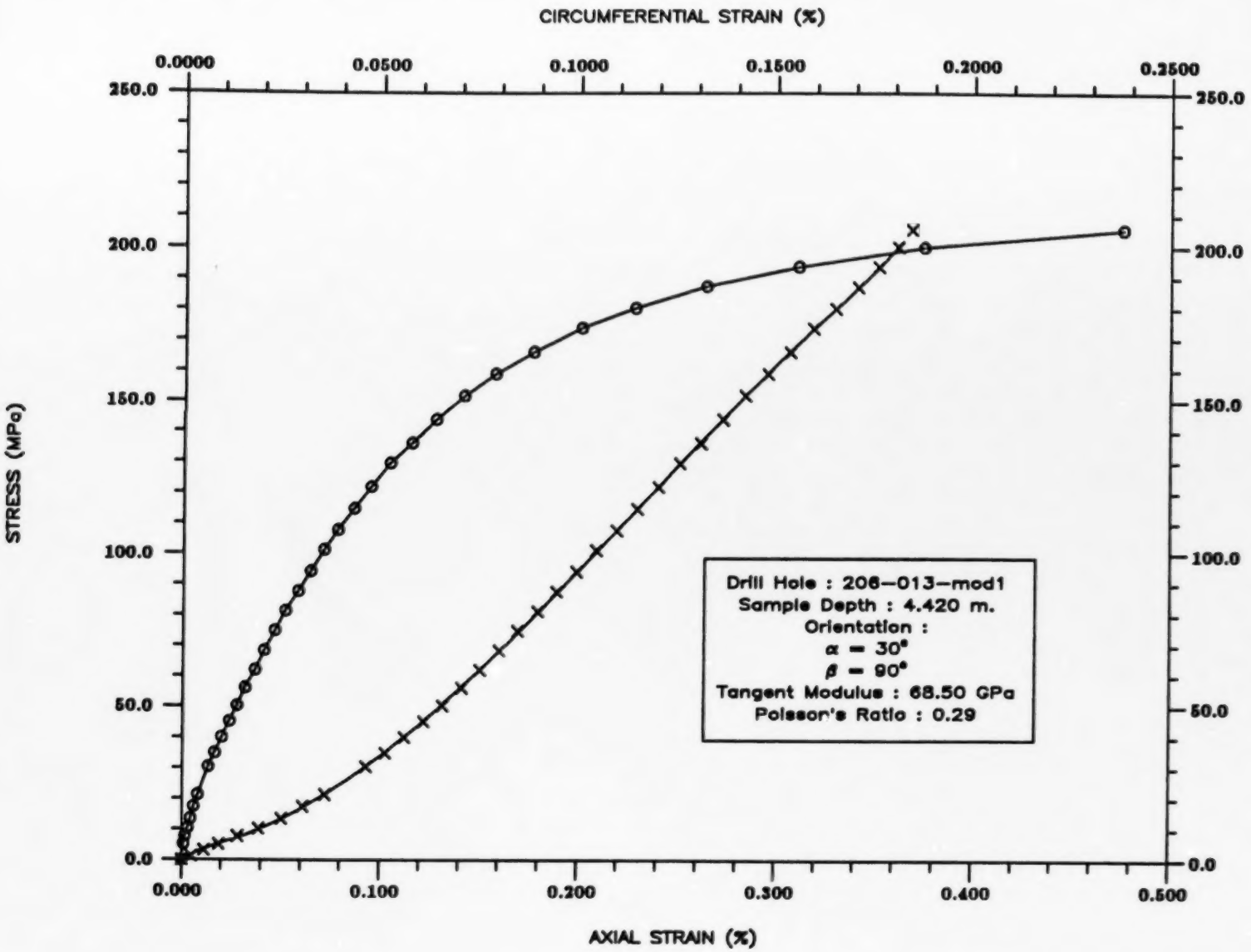

Fig. 3 : Axial and circumferential stress/strain curves for anisotropy test specimens.

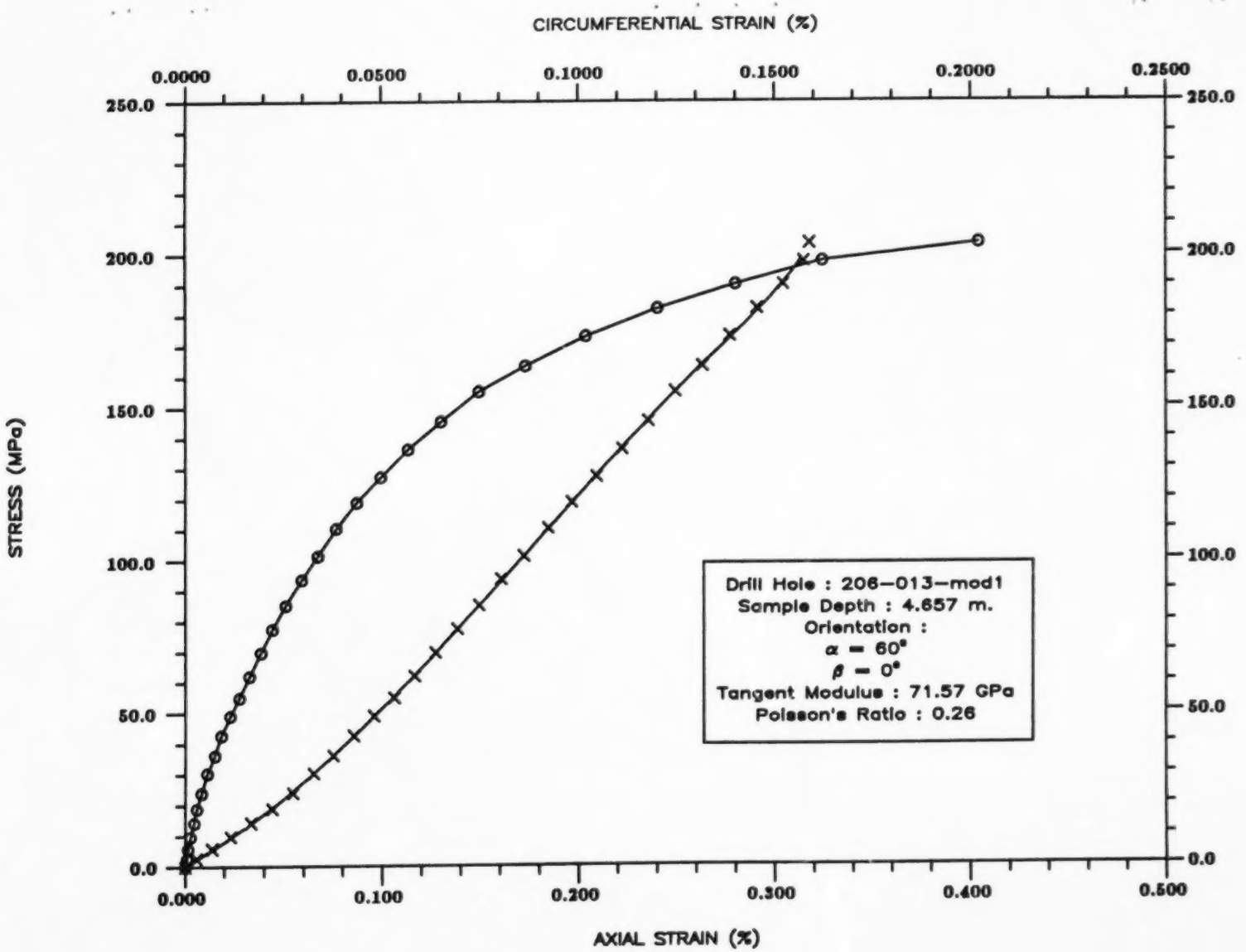

Fig. 4 : Axial and circumferential stress/strain curves for anisotropy test specimens.

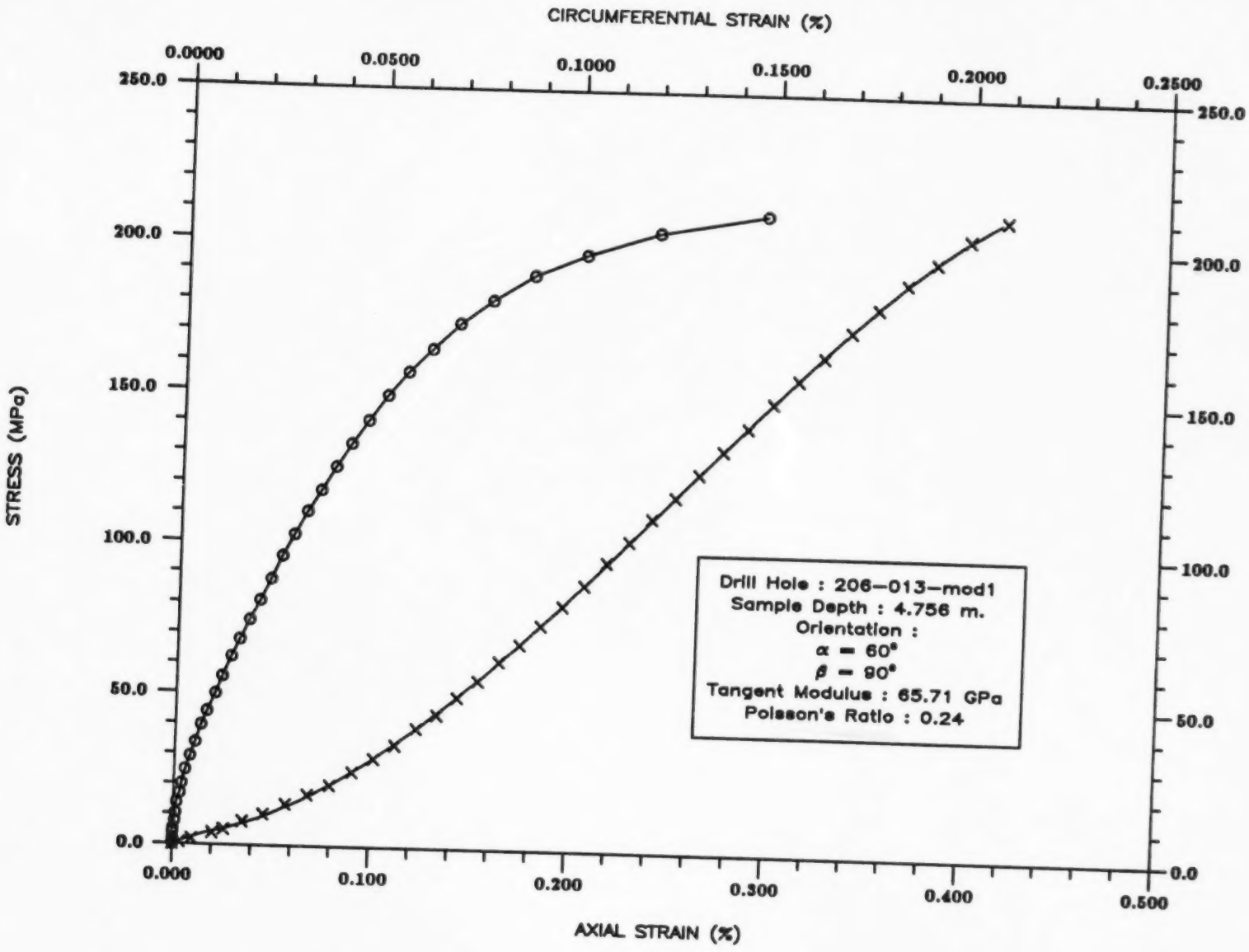

Fig. 5 : Axial and circumferential stress/strain curves for anisotropy test specimens.

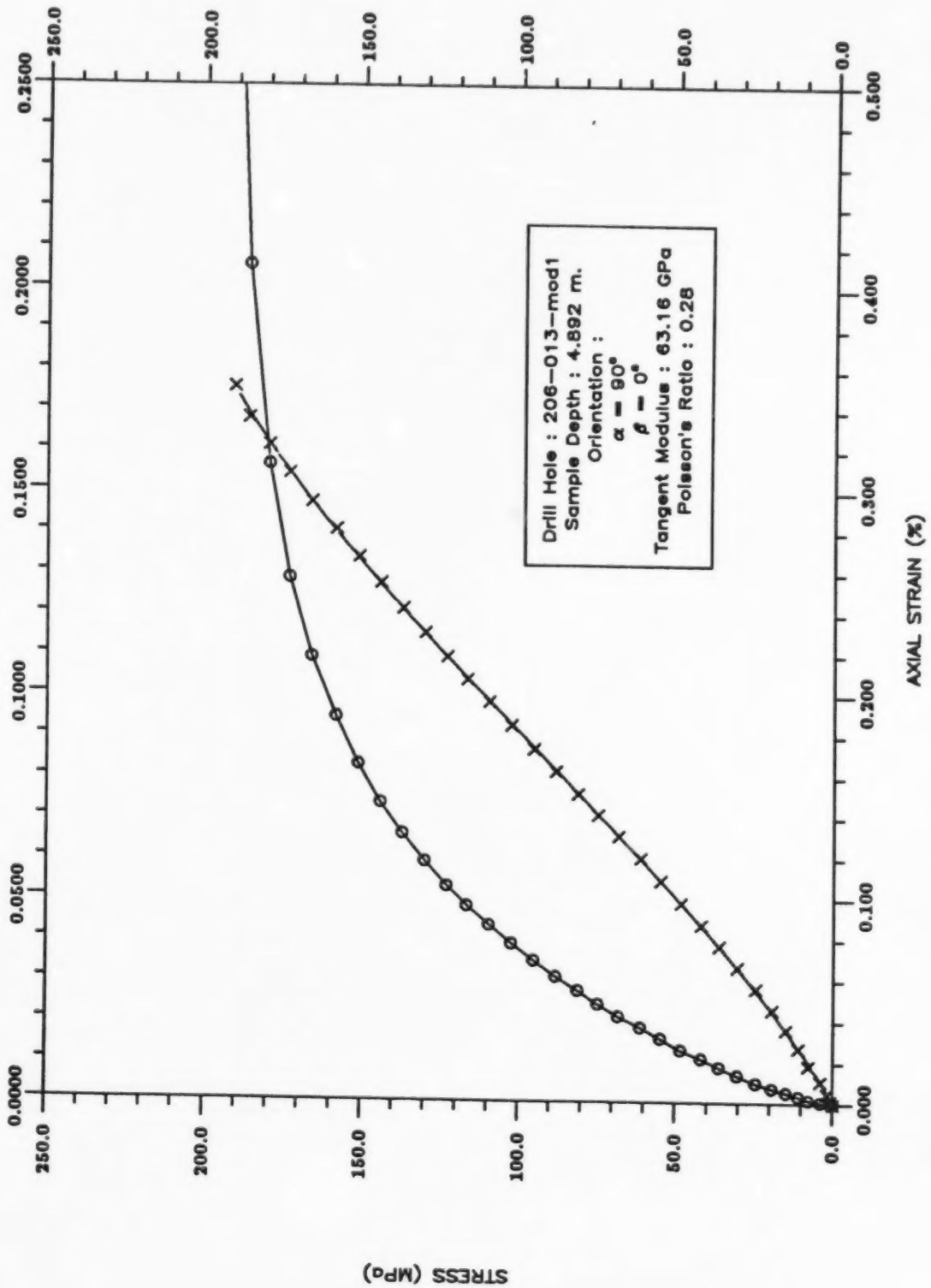

Fig. 6 : Axial and circumferential stress/strain curves for anisotropy test specimens.

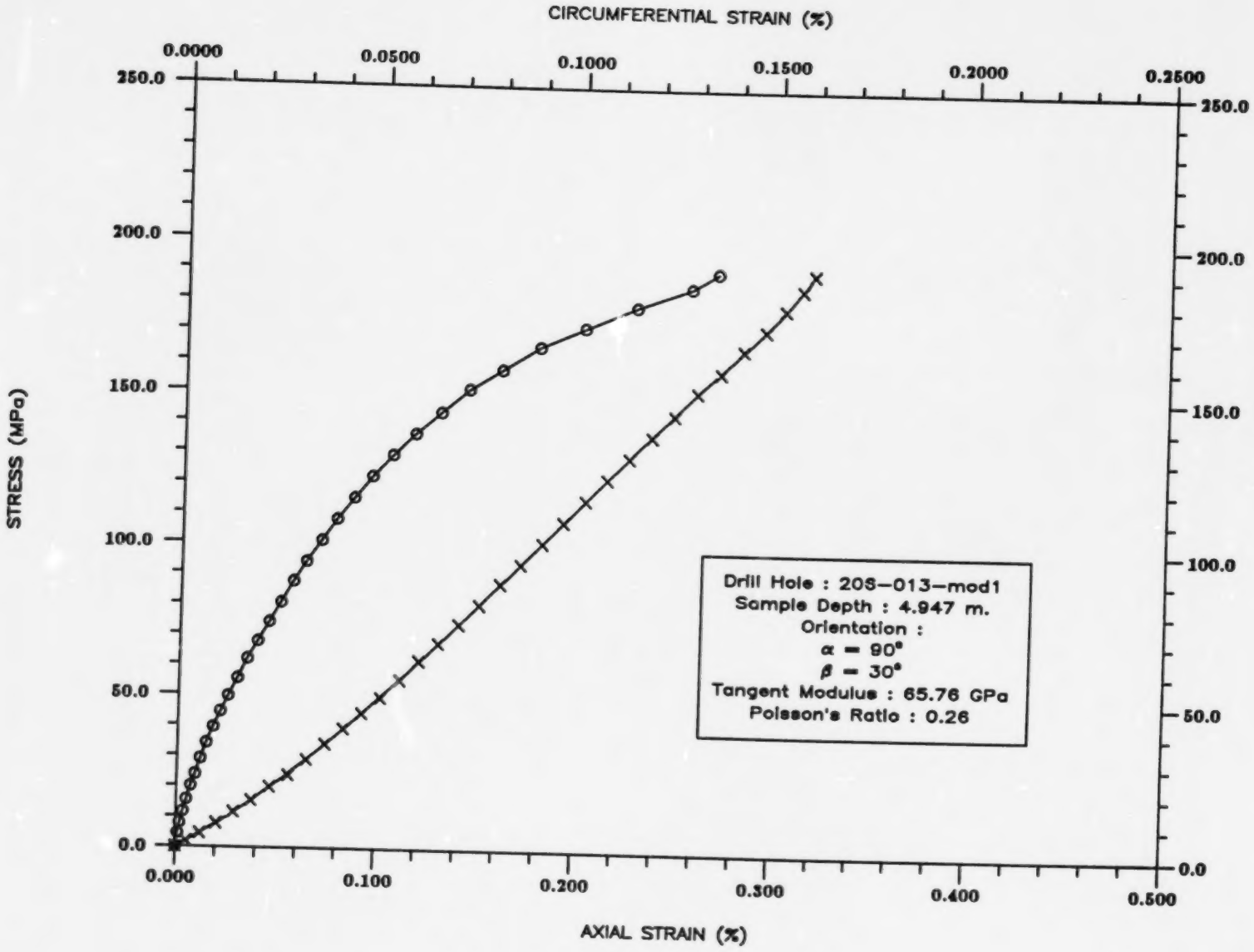

Fig. 7 : Axial and circumferential stress/strain curves for anisotropy test specimens.

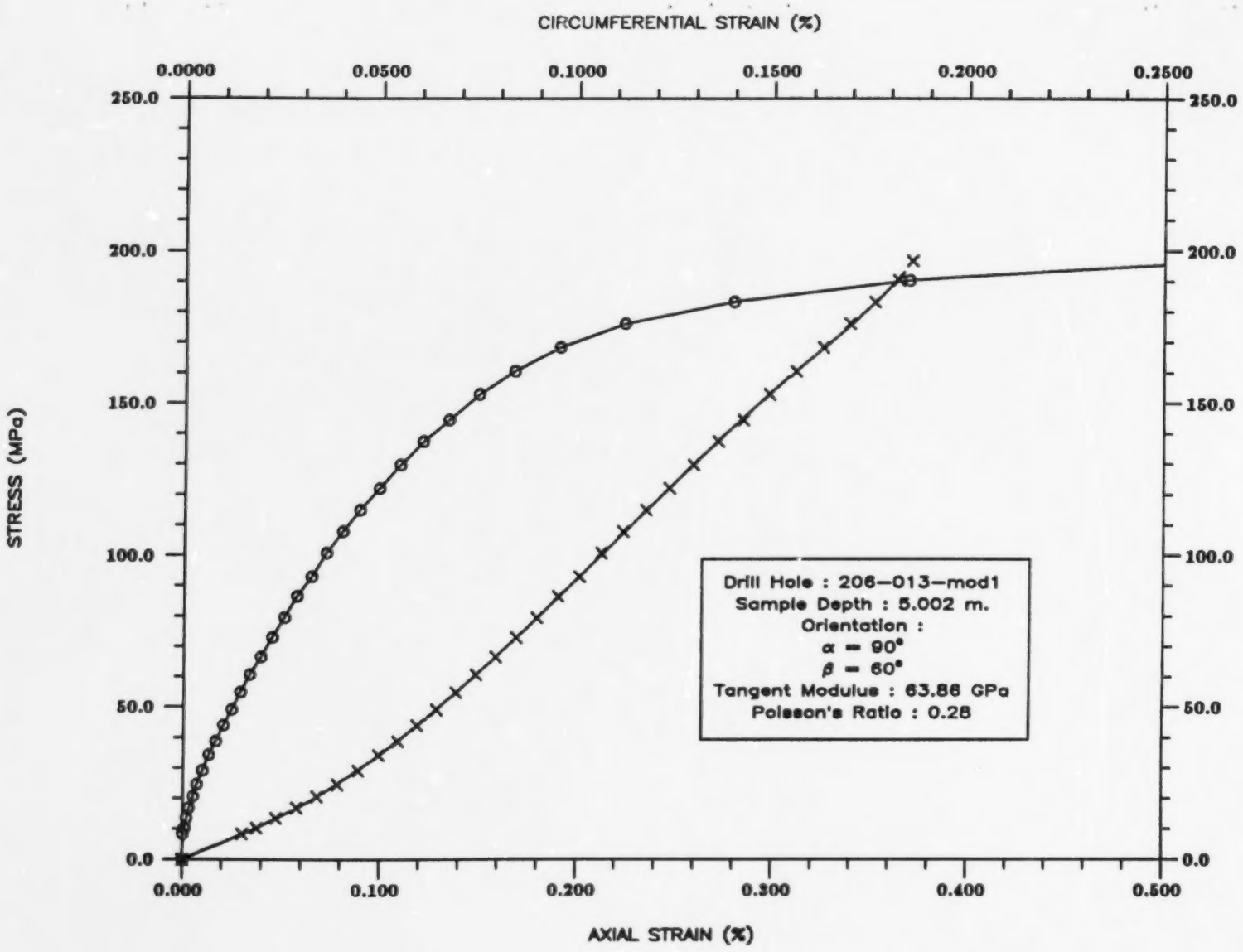

Fig. 8 : Axial and circumferential stress/strain curves for anisotropy test specimens.

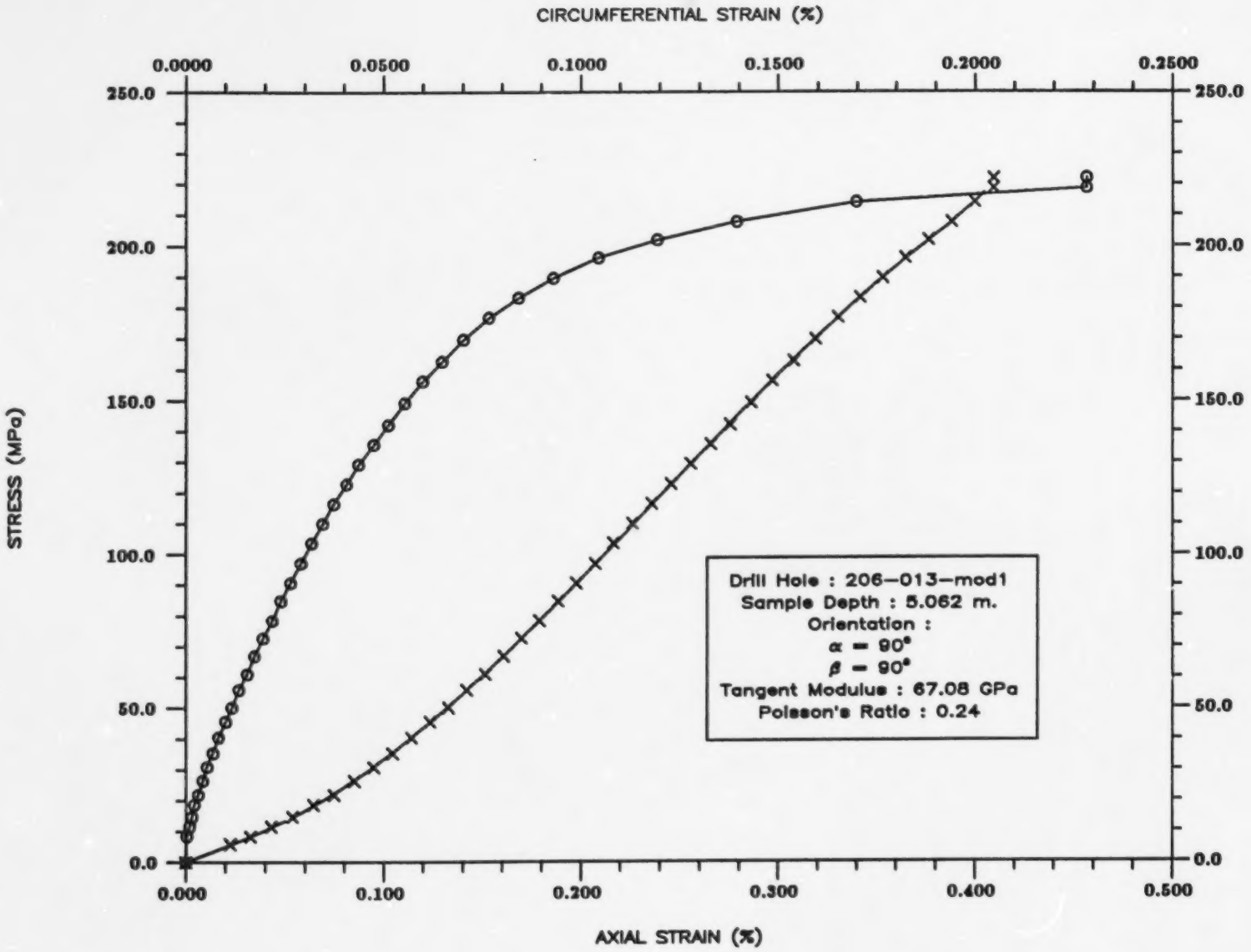

Fig. 9 : Axial and circumferential stress/strain curves for anisotropy test specimens.

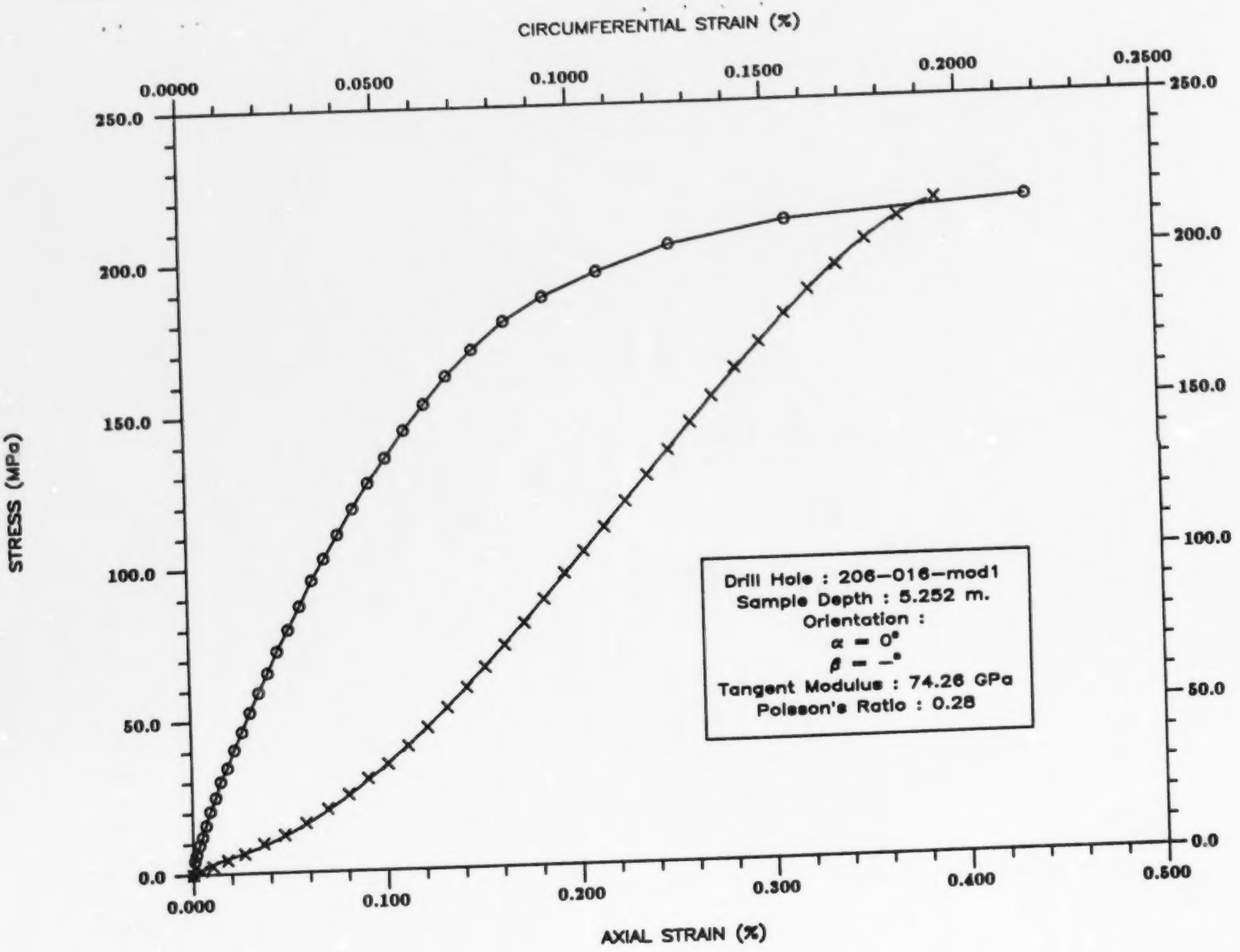

Fig. 10: Axial and circumferential stress/strain curves for anisotropy test specimens.

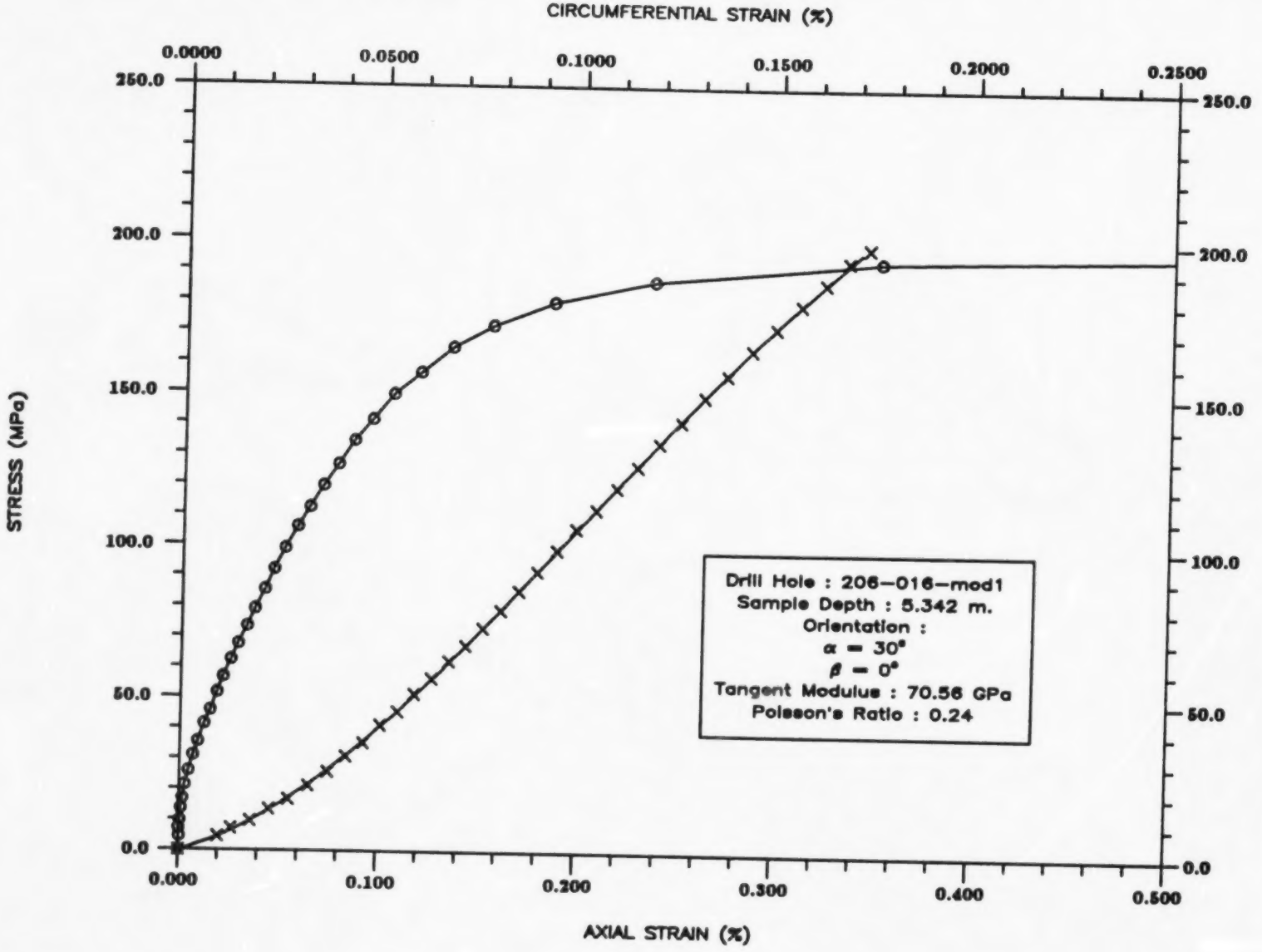

Fig. 11 : Axial and circumferential stress/strain curves for anisotropy test specimens.

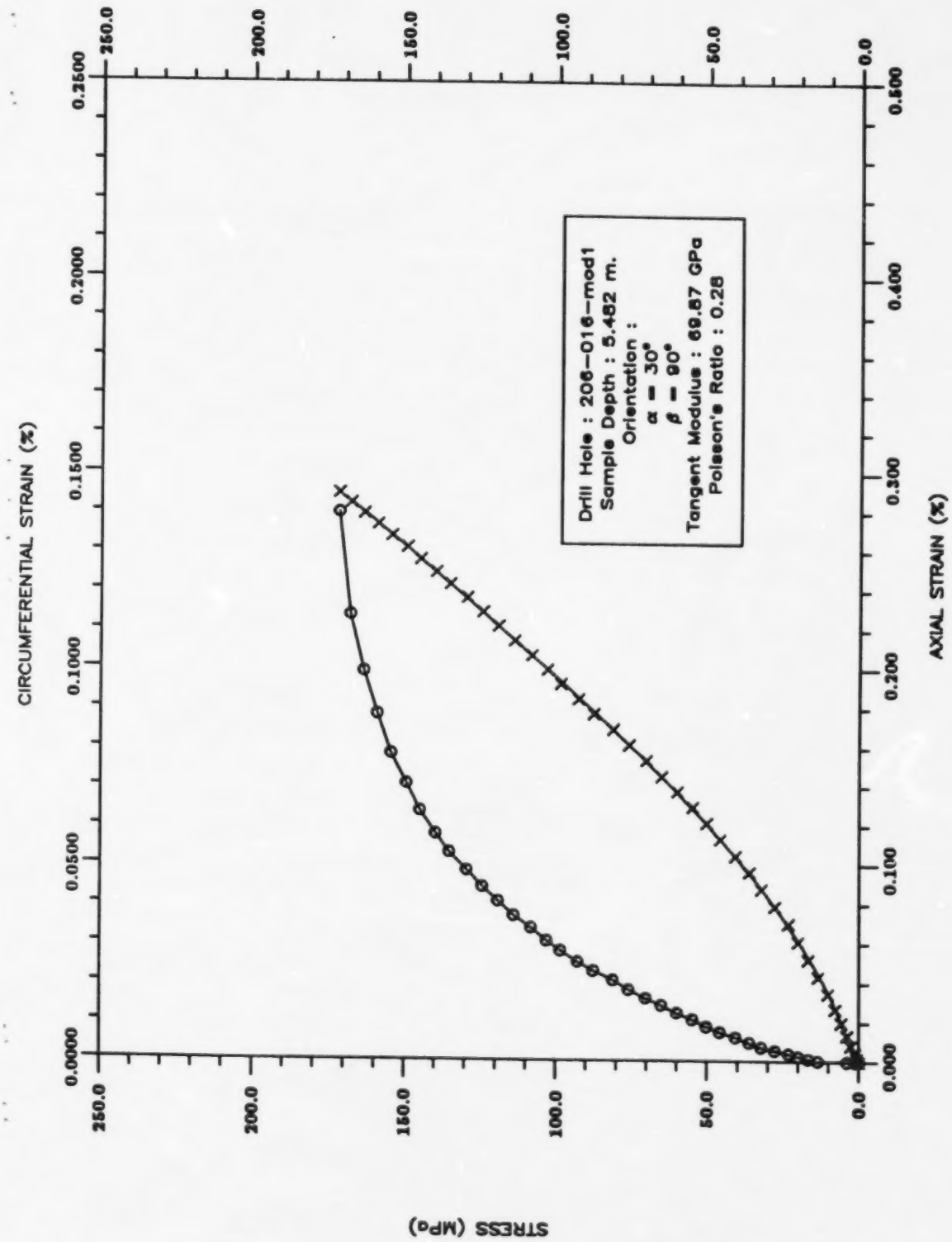

Fig. 12 : Axial and circumferential stress/strain curves for anisotropy test specimens.

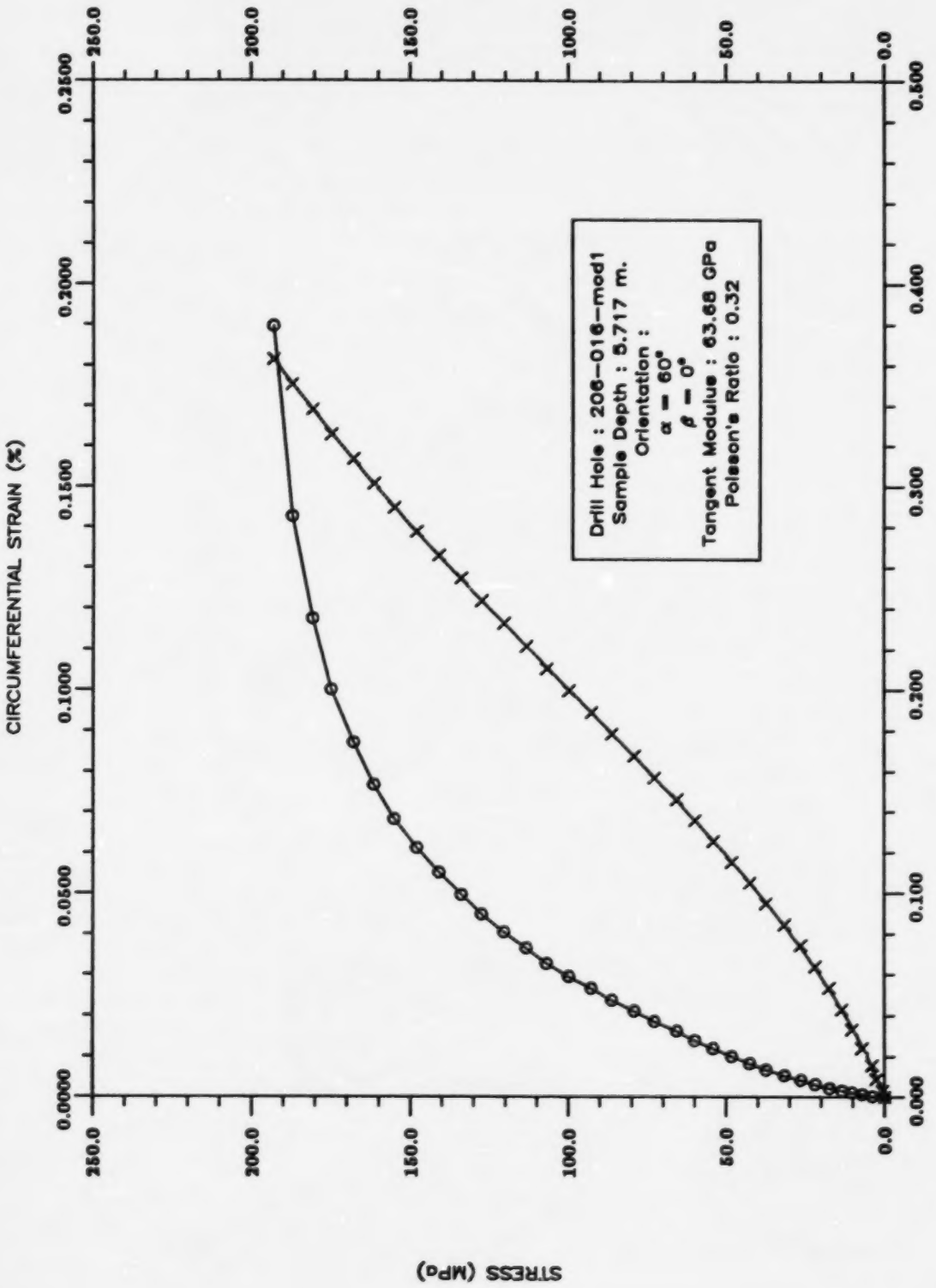

Fig. 13 : Axial and circumferential stress/strain curves for anisotropy test specimens.

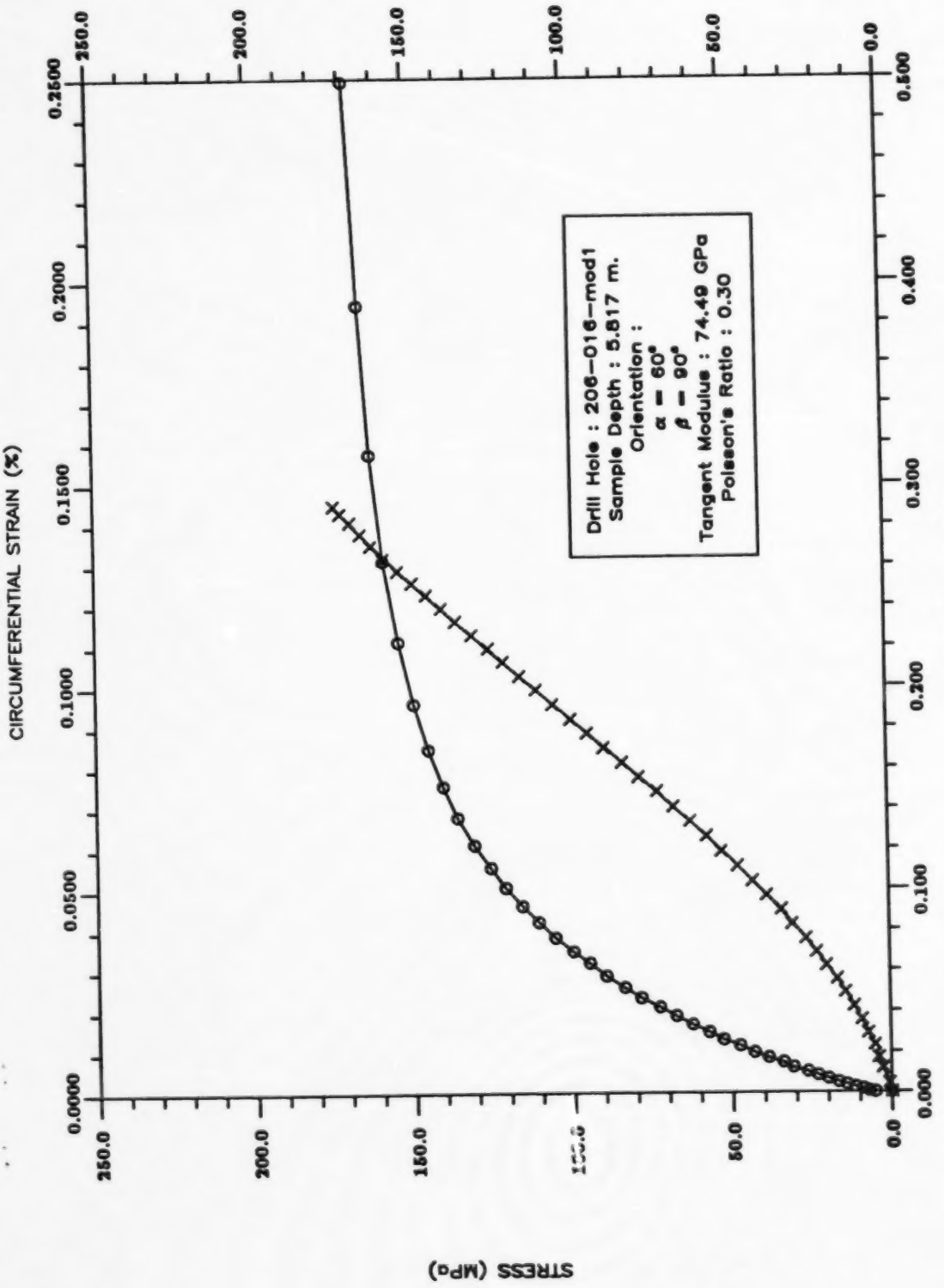

Fig. 14 : Axial and circumferential stress/strain curves for anisotropy test specimens.

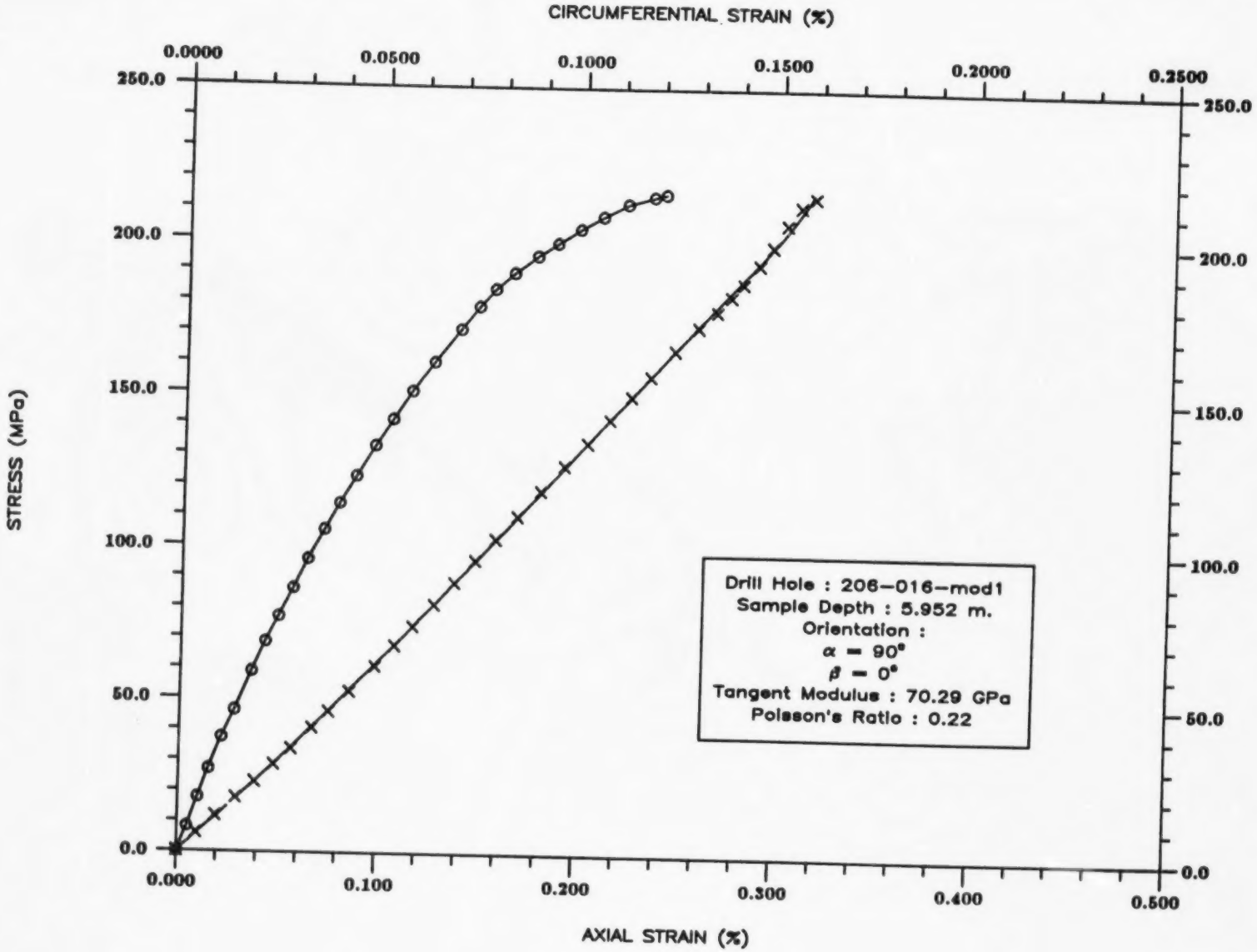

Fig. 15 : Axial and circumferential stress/strain curves for anisotropy test specimens.

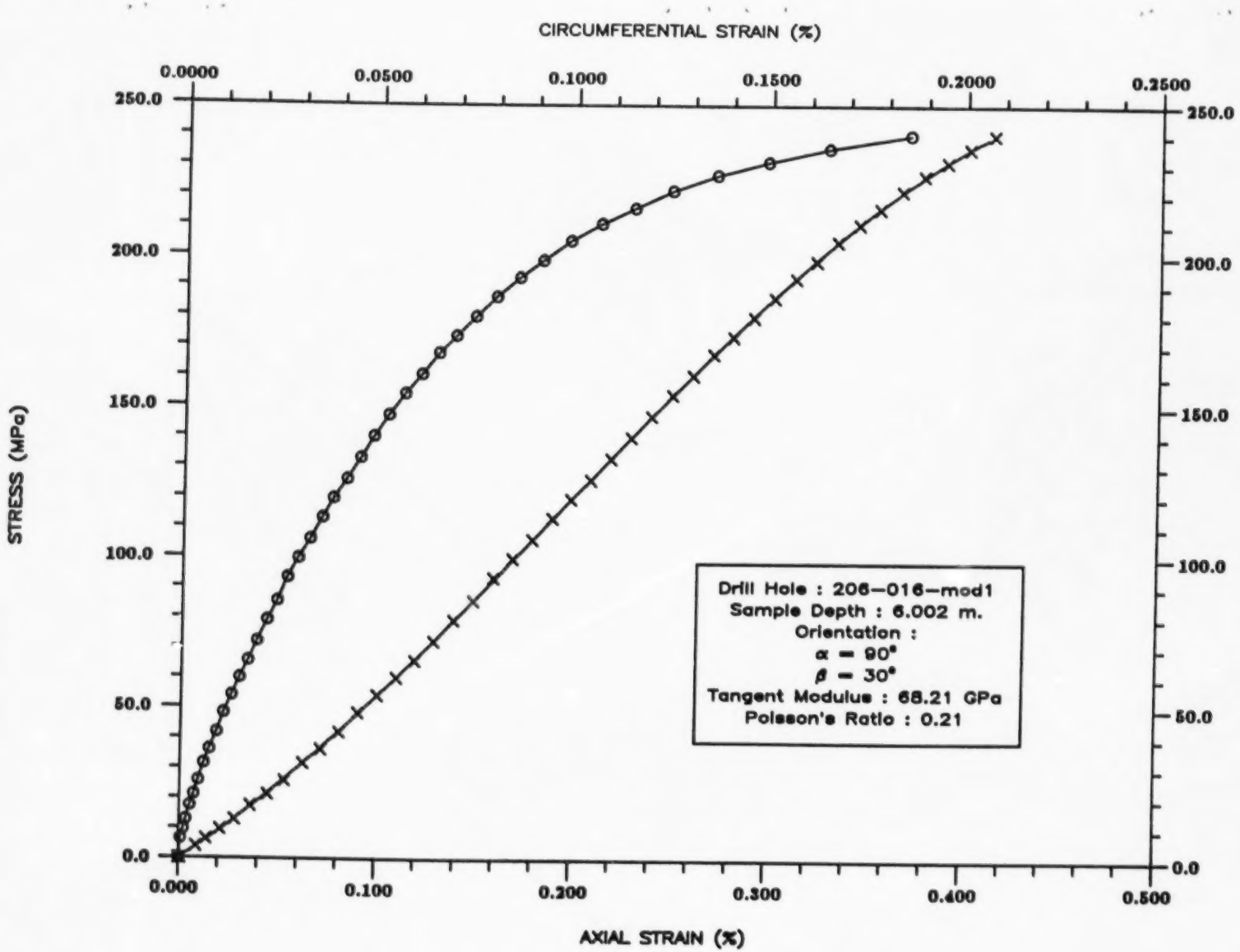

Fig. 16 : Axial and circumferential stress/strain curves for anisotropy test specimens.

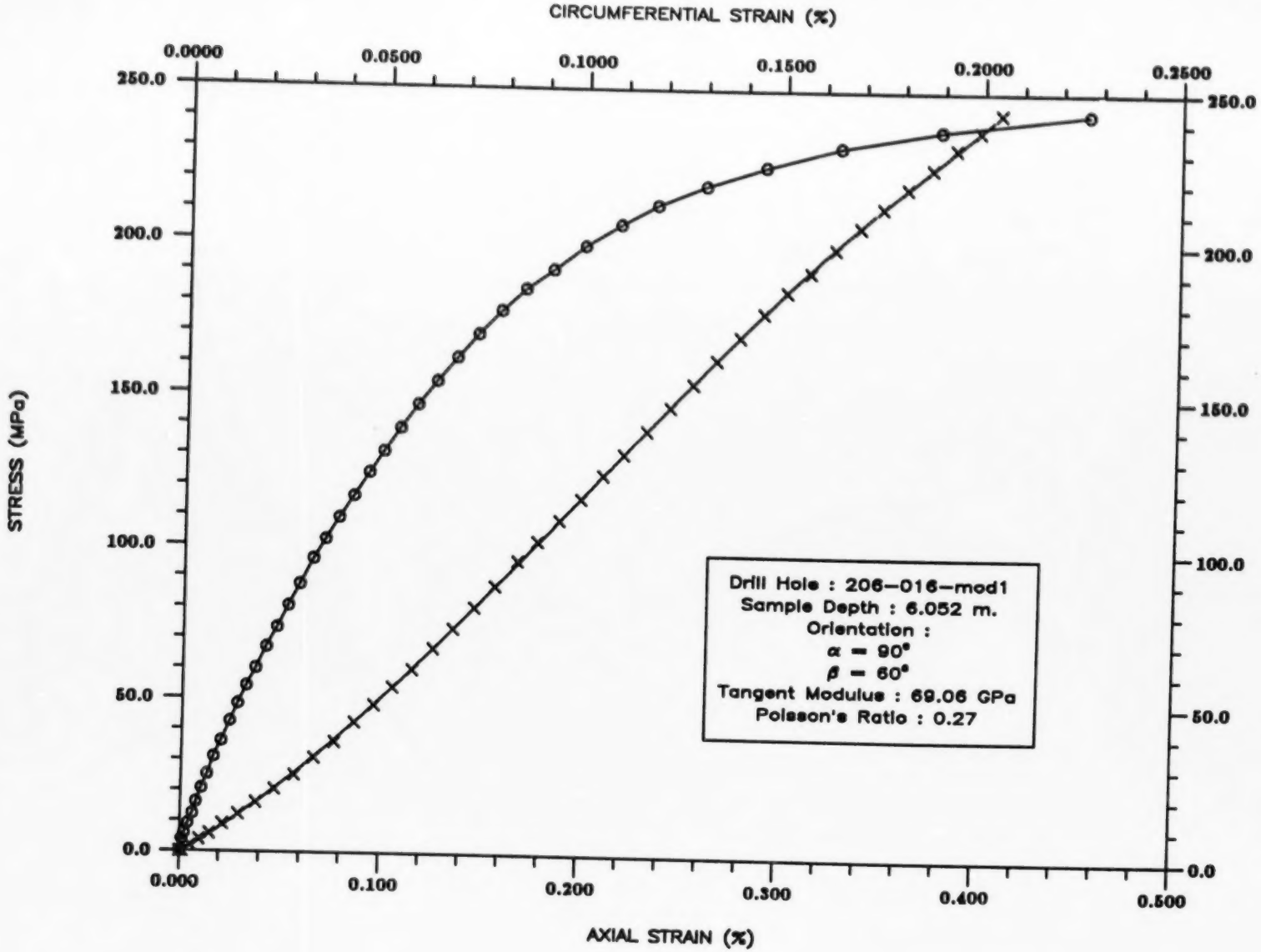

Fig. 17 : Axial and circumferential stress/strain curves for anisotropy test specimens.

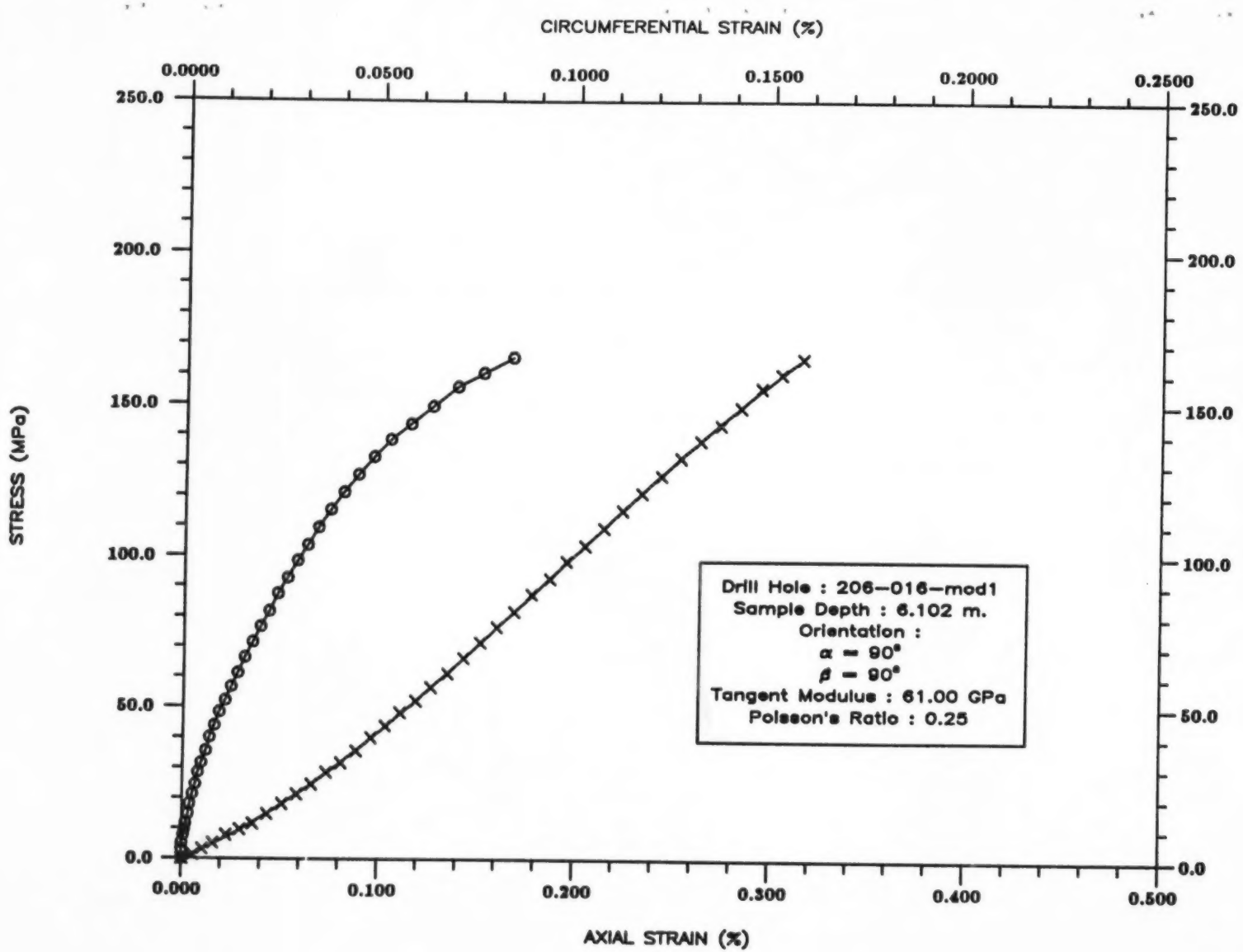

Fig. 18 : Axial and circumferential stress/strain curves for anisotropy test specimens.

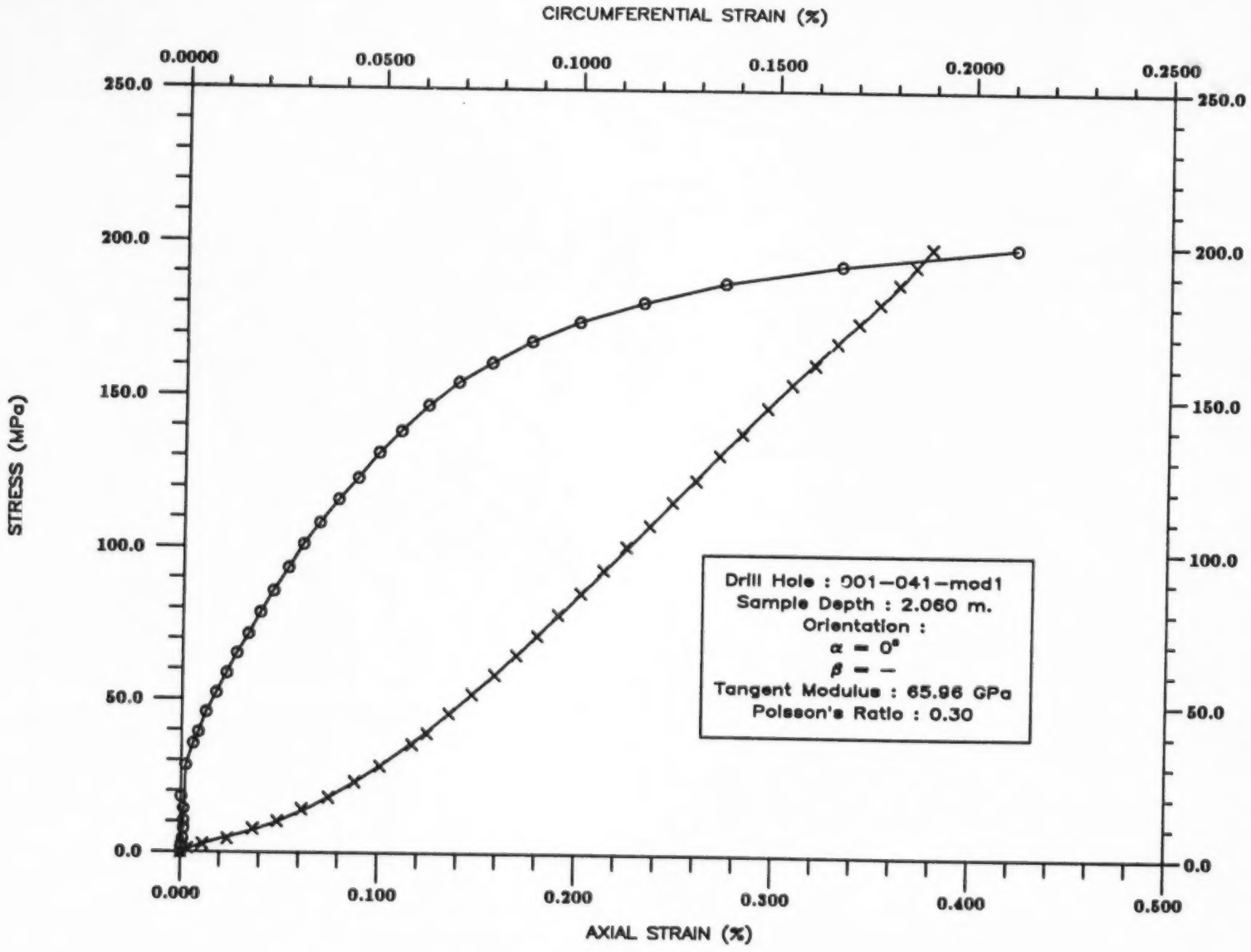

Fig. 19 : Axial and circumferential stress/strain curves for anisotropy test specimens.

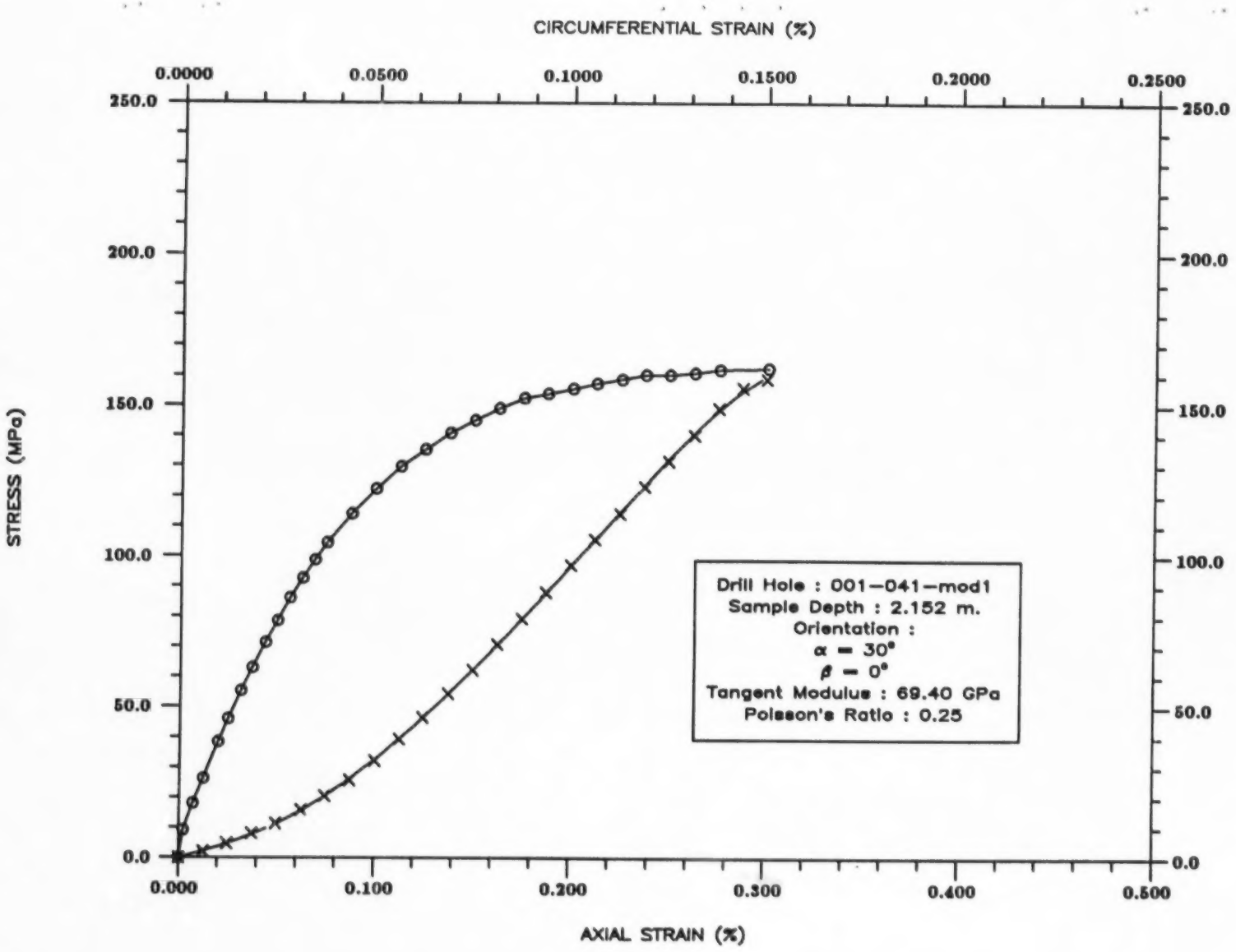

Fig. 20: Axial and circumferential stress/strain curves for anisotropy test specimens.

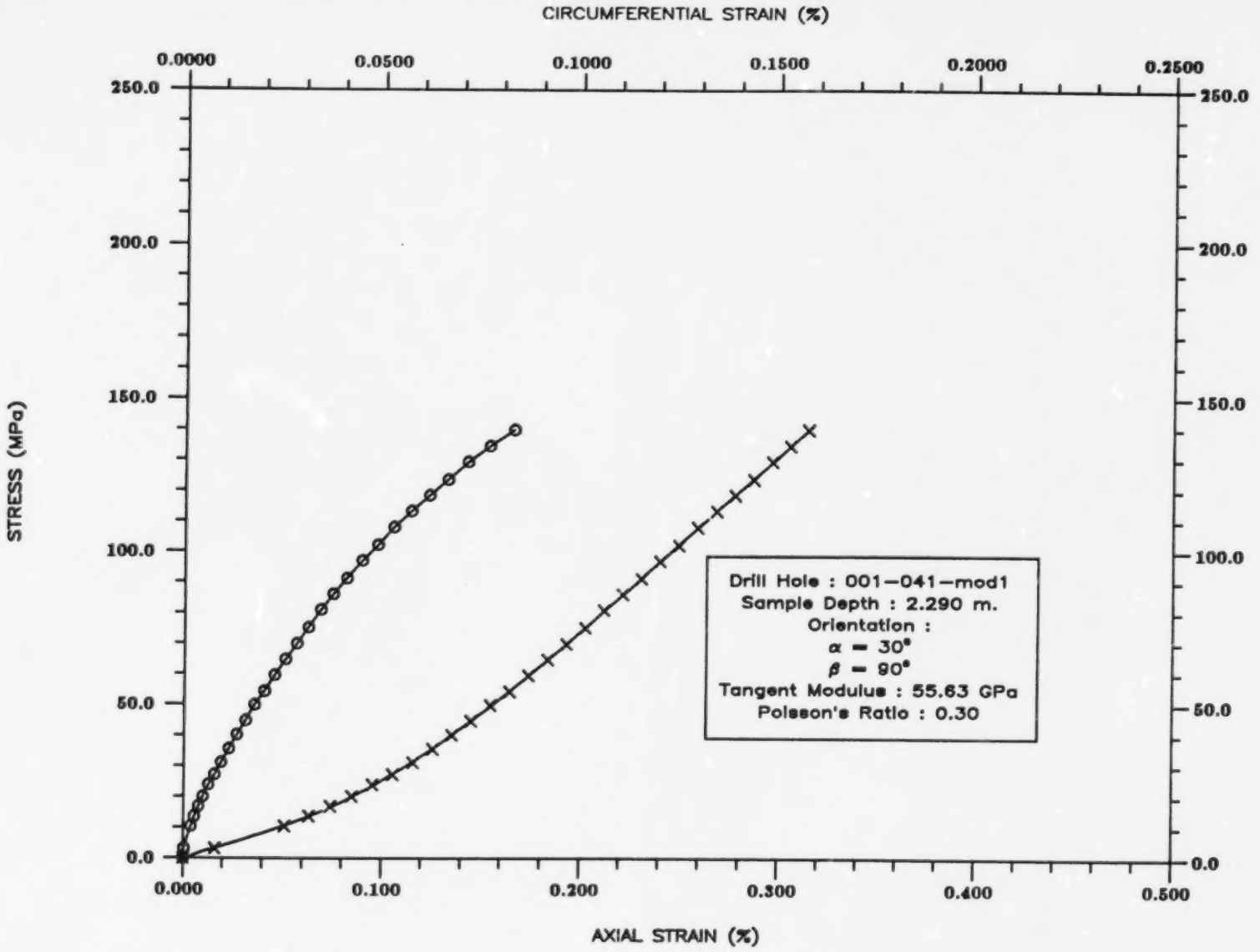

Fig. 21 : Axial and circumferential stress/strain curves for anisotropy test specimens.

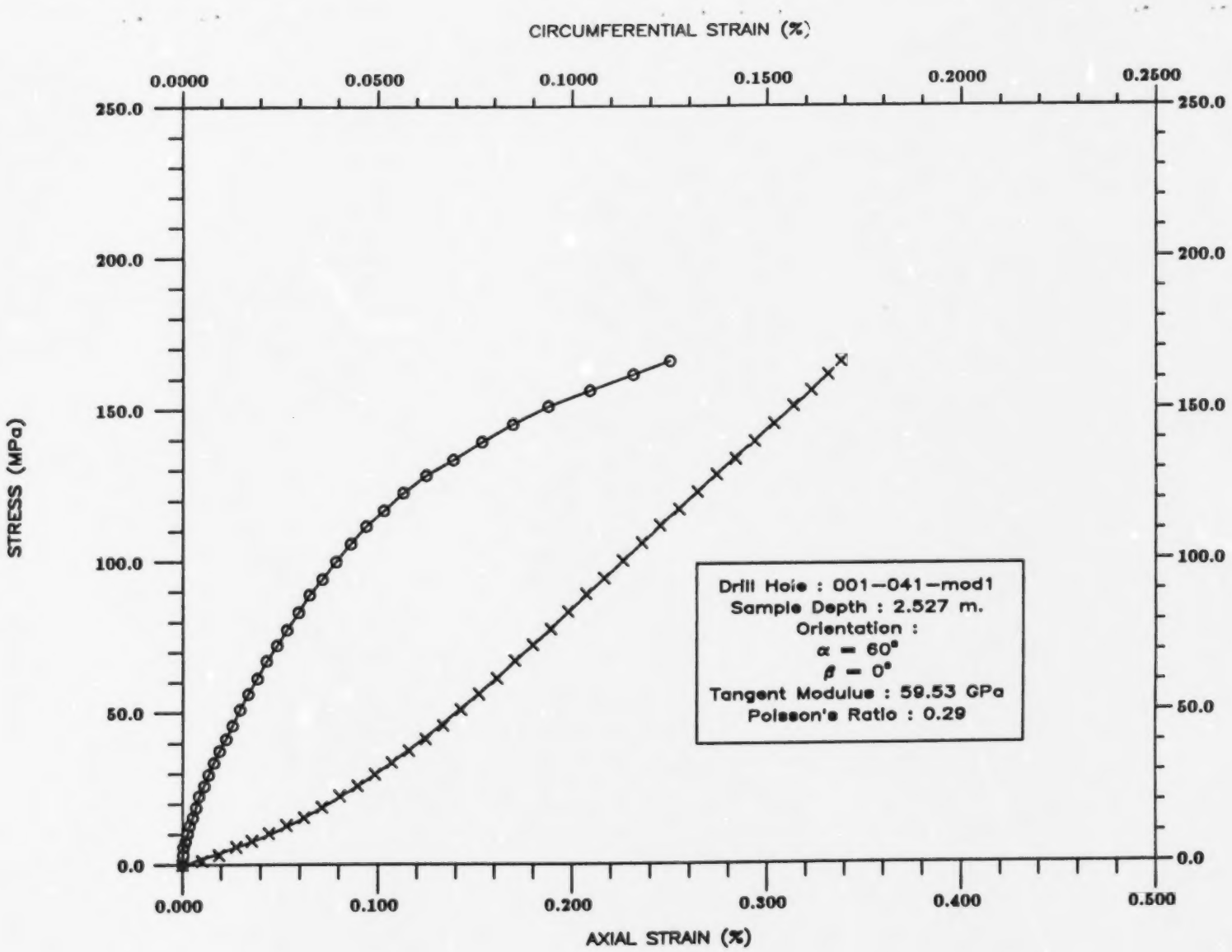

Fig. 22: Axial and circumferential stress/strain curves for anisotropy test specimens.

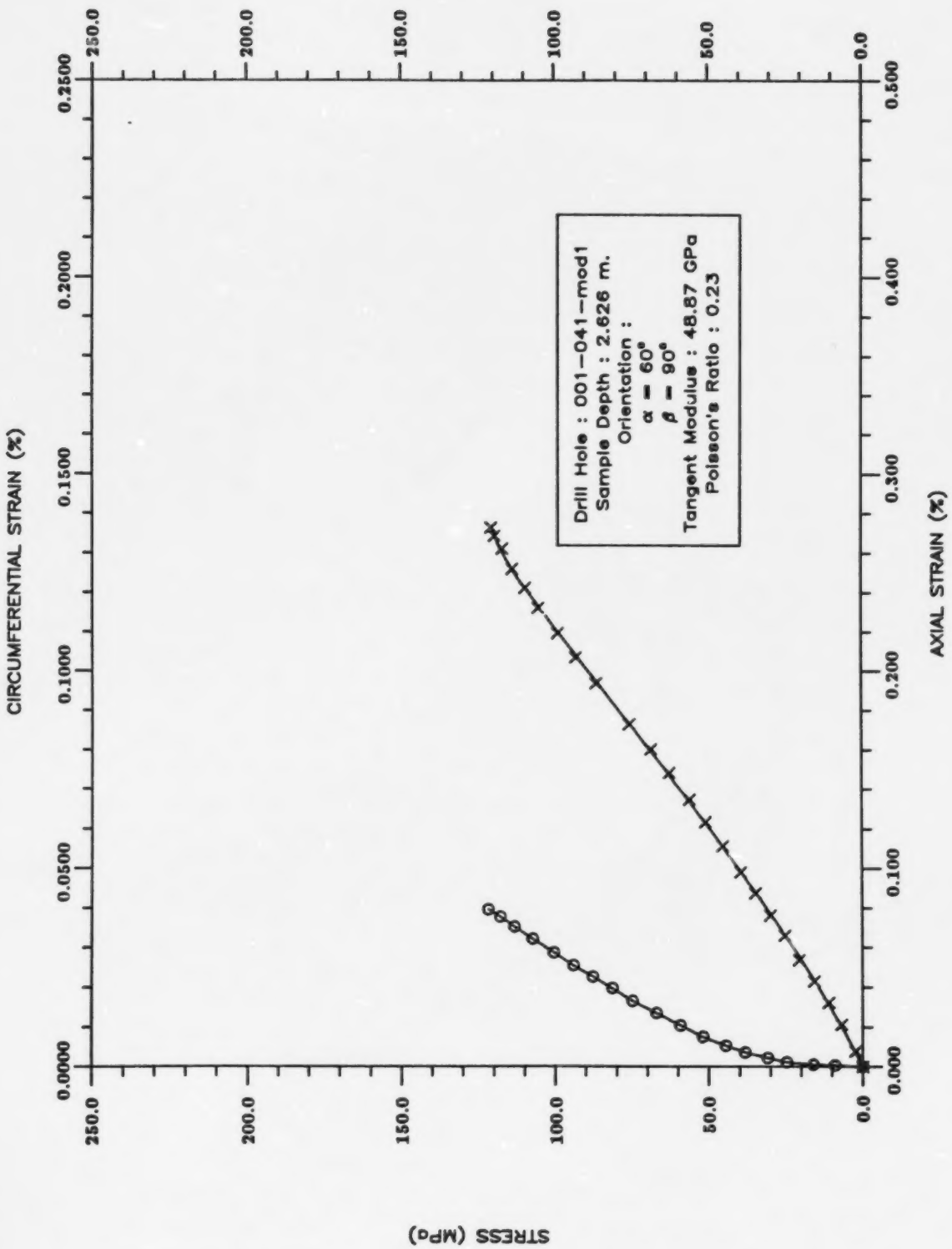

Fig. 23: Axial and circumferential stress/strain curves for anisotropy test specimens.

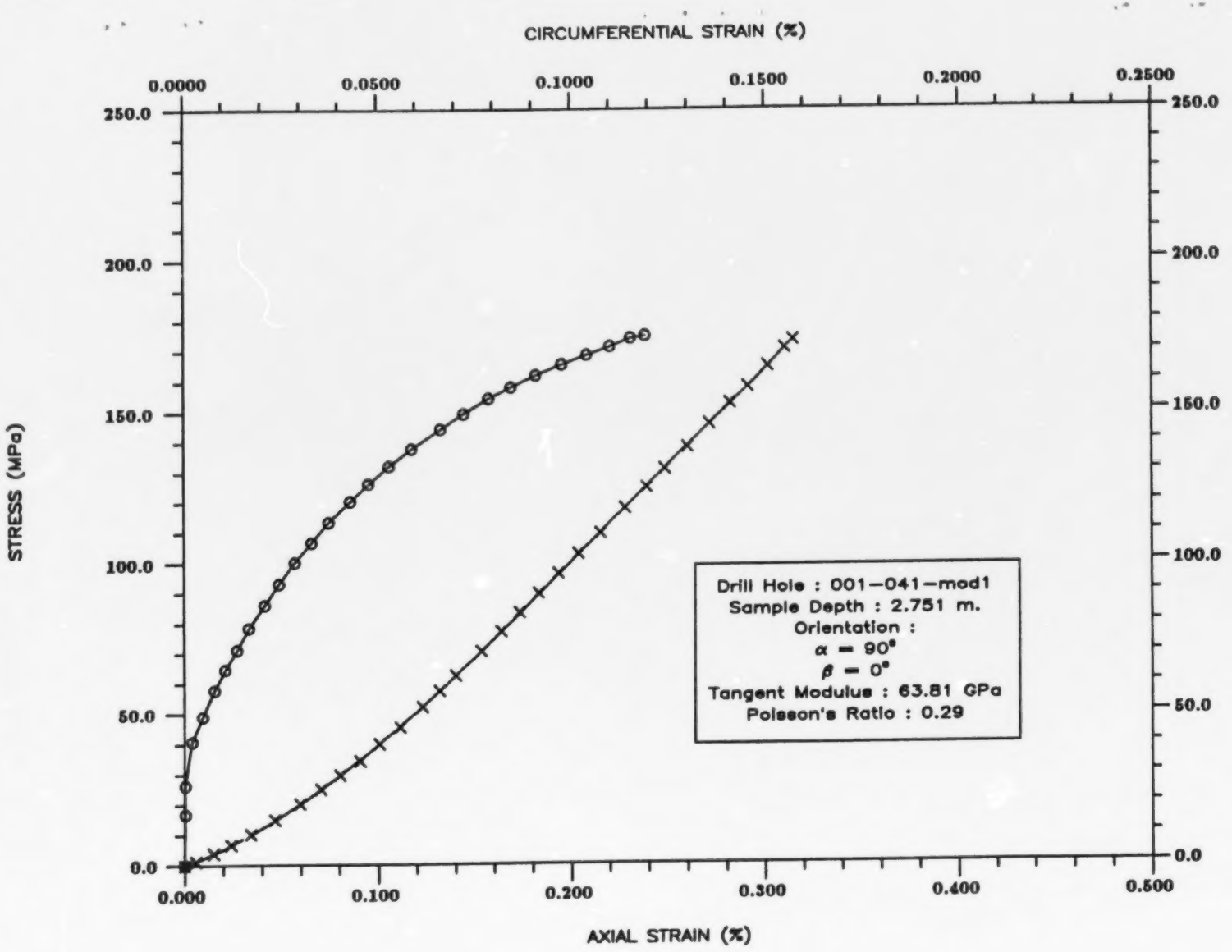

Fig. 24: Axial and circumferential stress/strain curves for anisotropy test specimens.

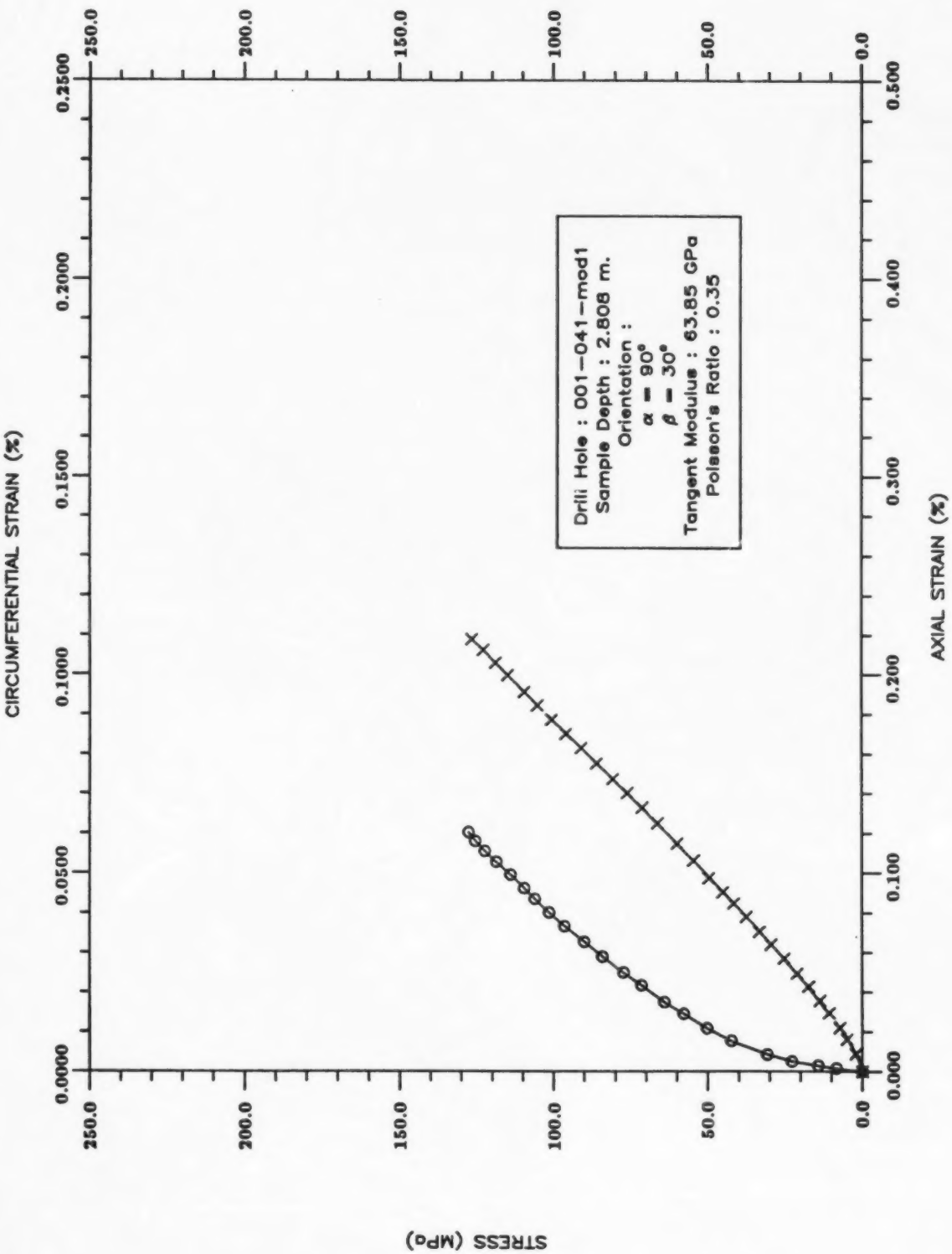

Fig. 25: Axial and circumferential stress/strain curves for anisotropy test specimens.

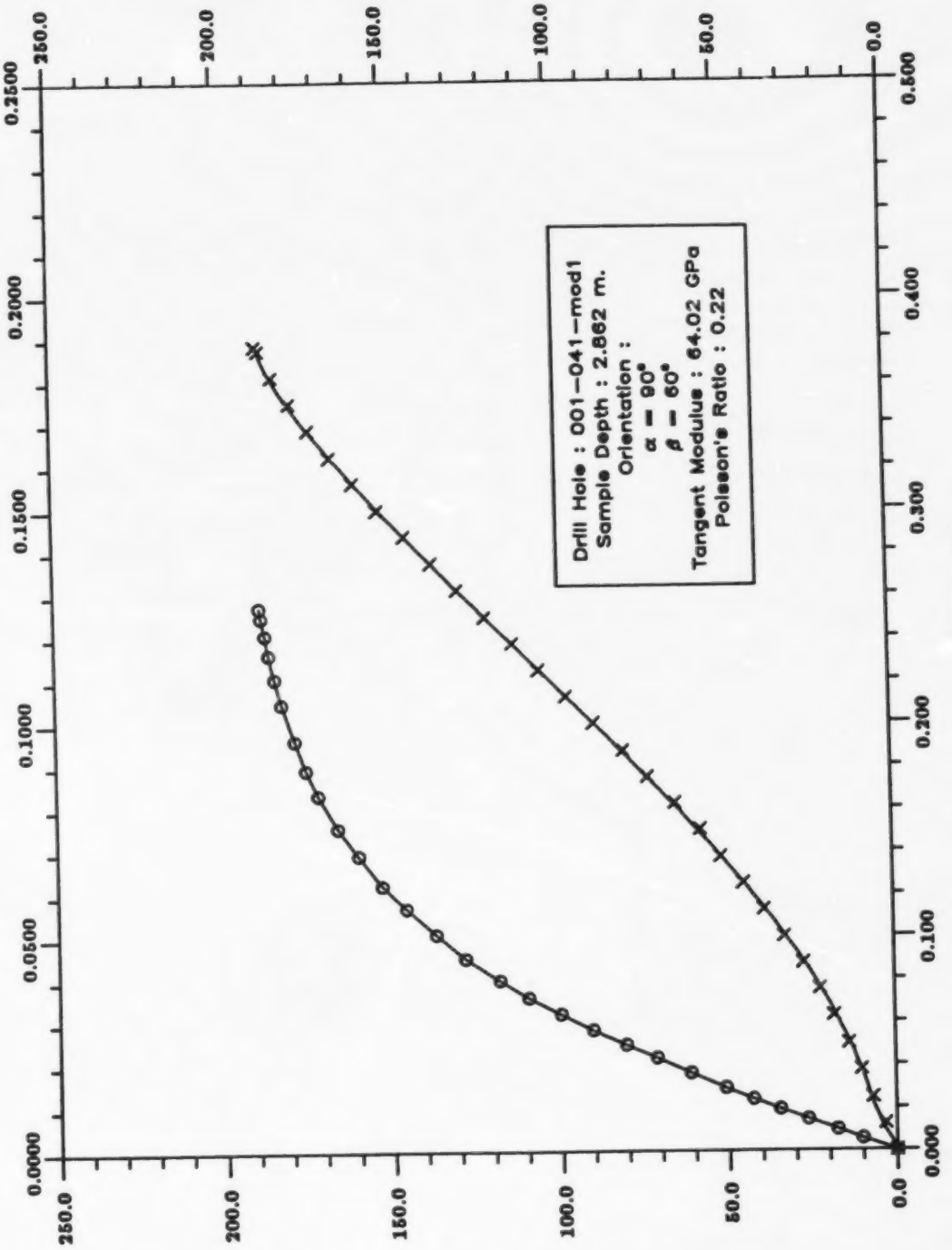

Fig. 26: Axial and circumferential stress/strain curves for anisotropy test specimens.

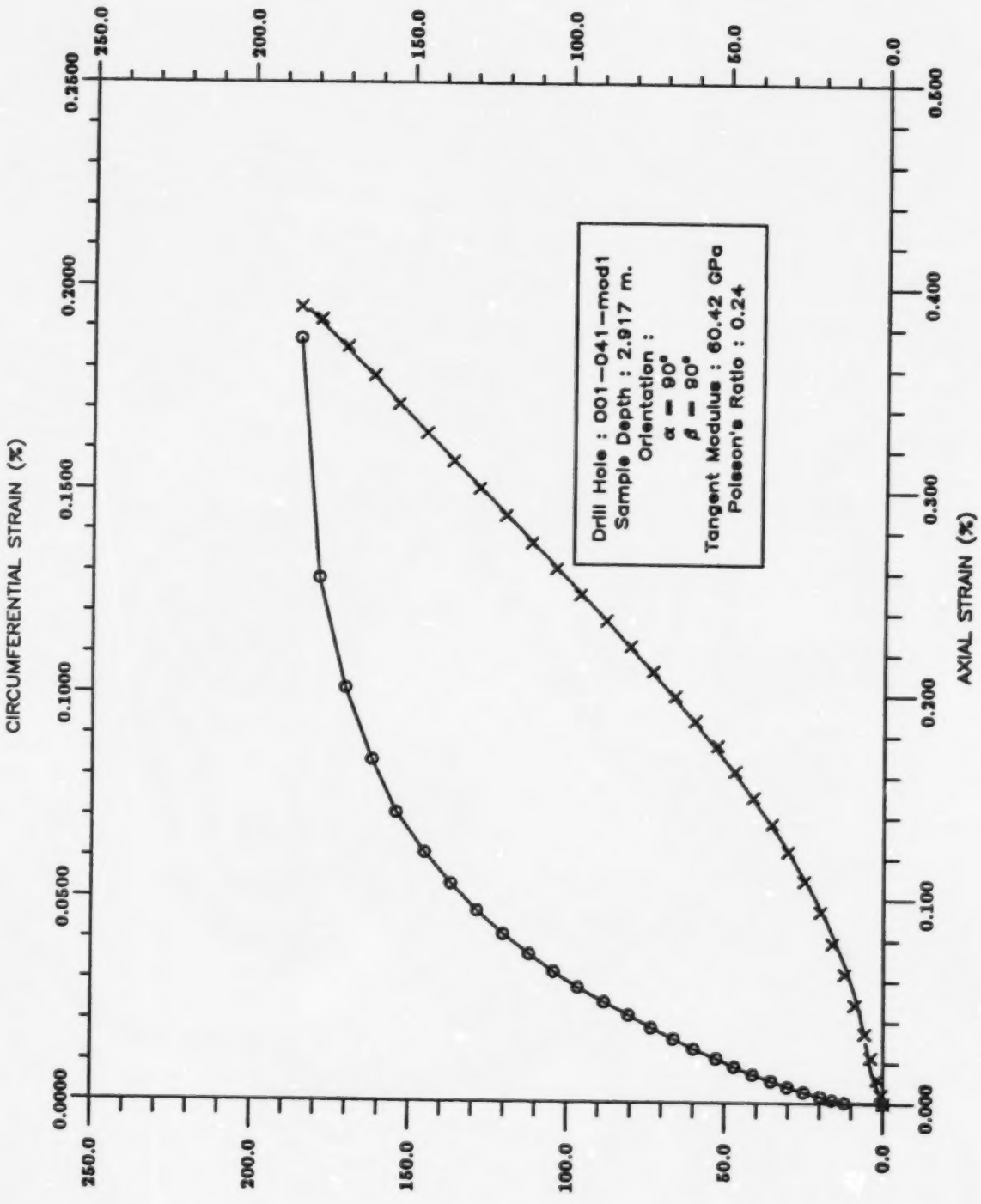

Fig. 27: Axial and circumferential stress/strain curves for anisotropy test specimens.

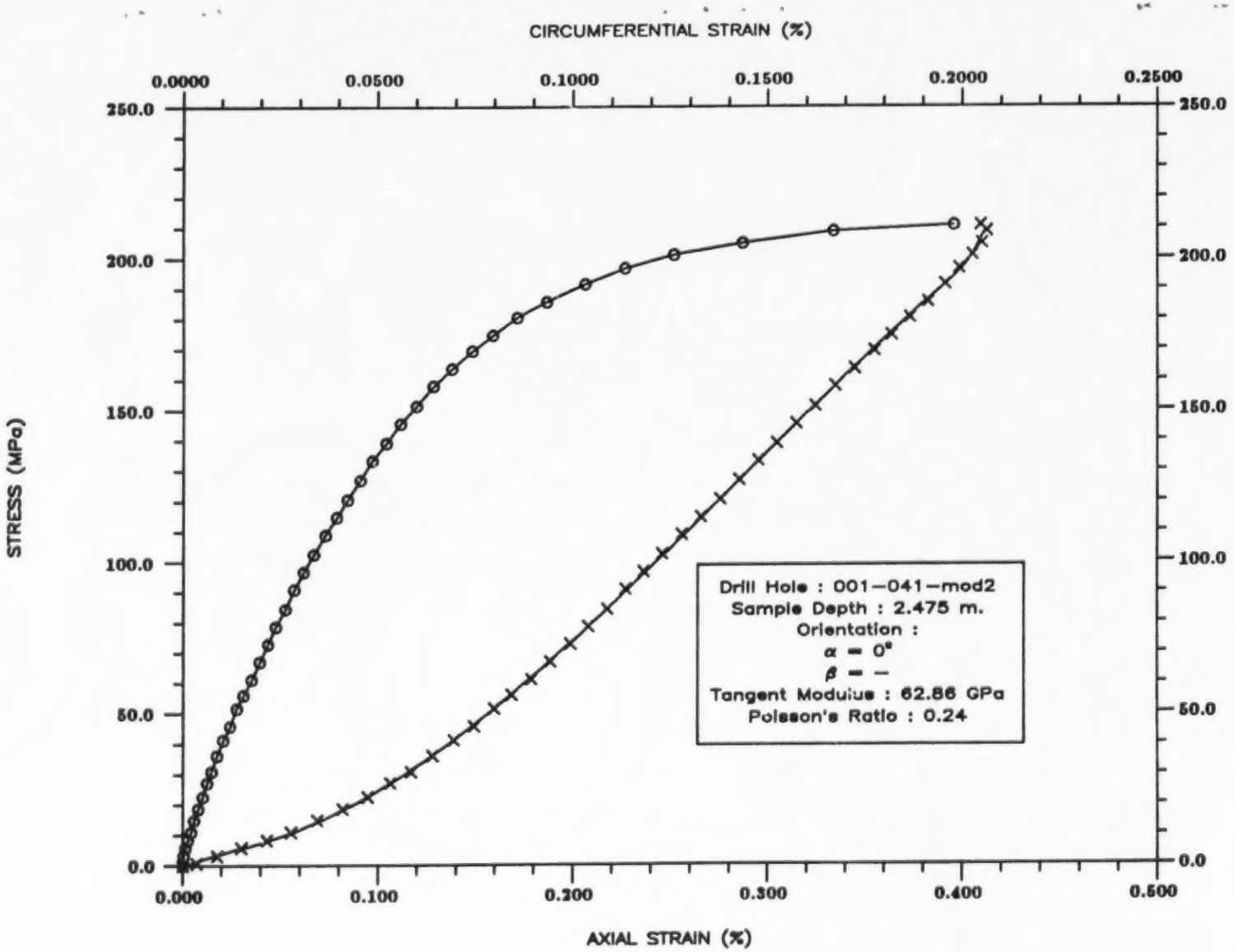

Fig. 28: Axial and circumferential stress/strain curves for anisotropy test specimens.

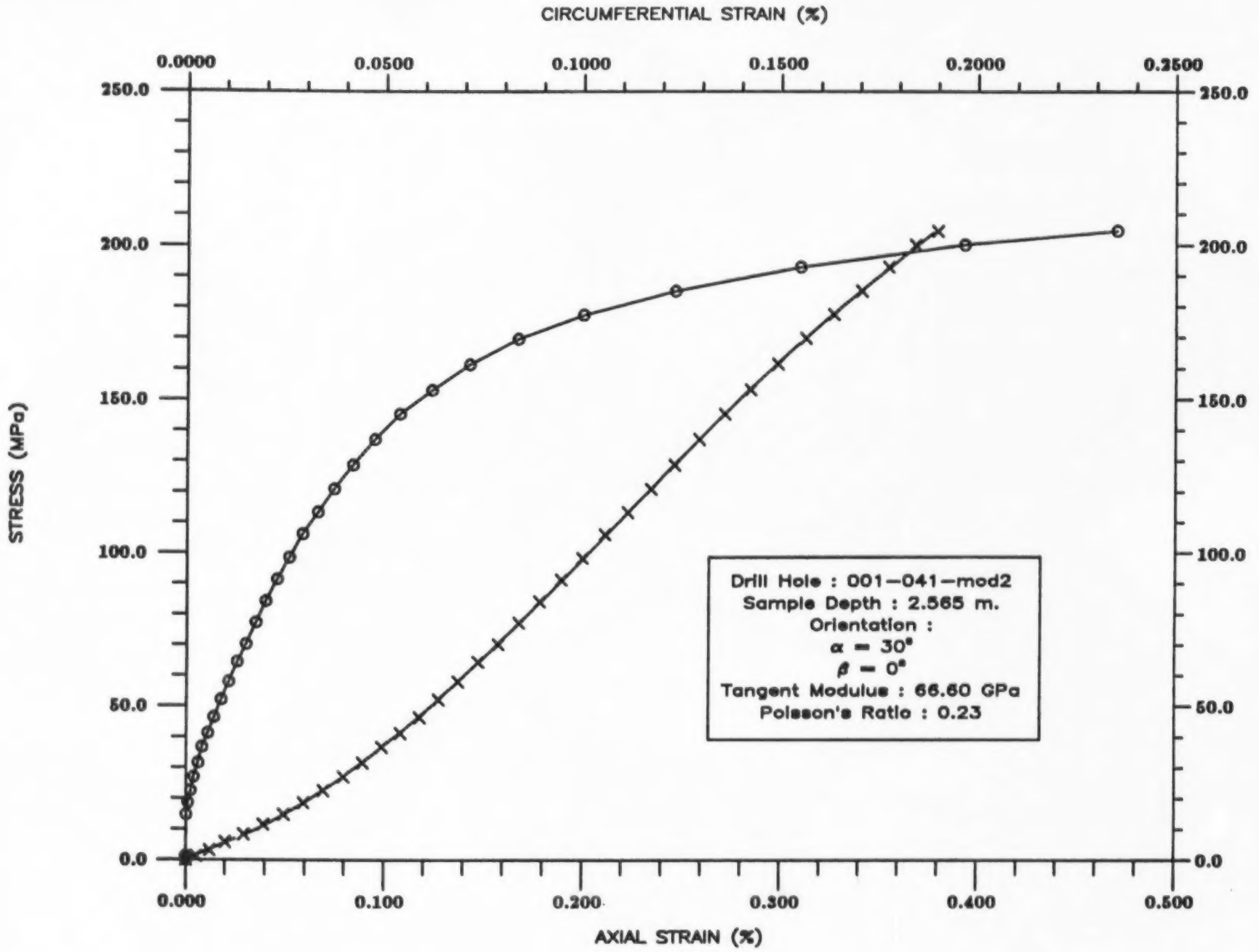

Fig. 29: Axial and circumferential stress/strain curves for anisotropy test specimens.

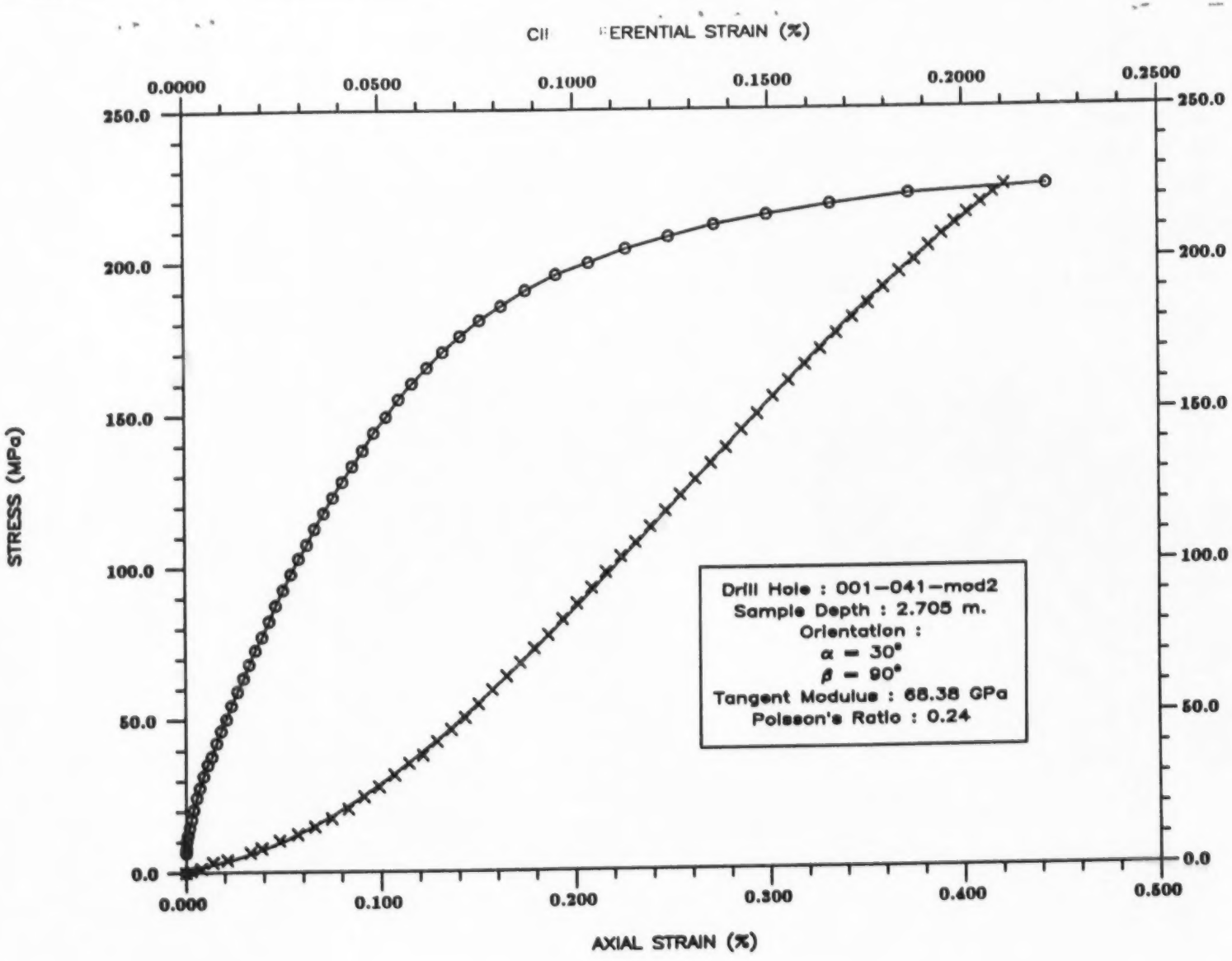

Fig. 30: Axial and circumferential stress/strain curves for anisotropy test specimens.

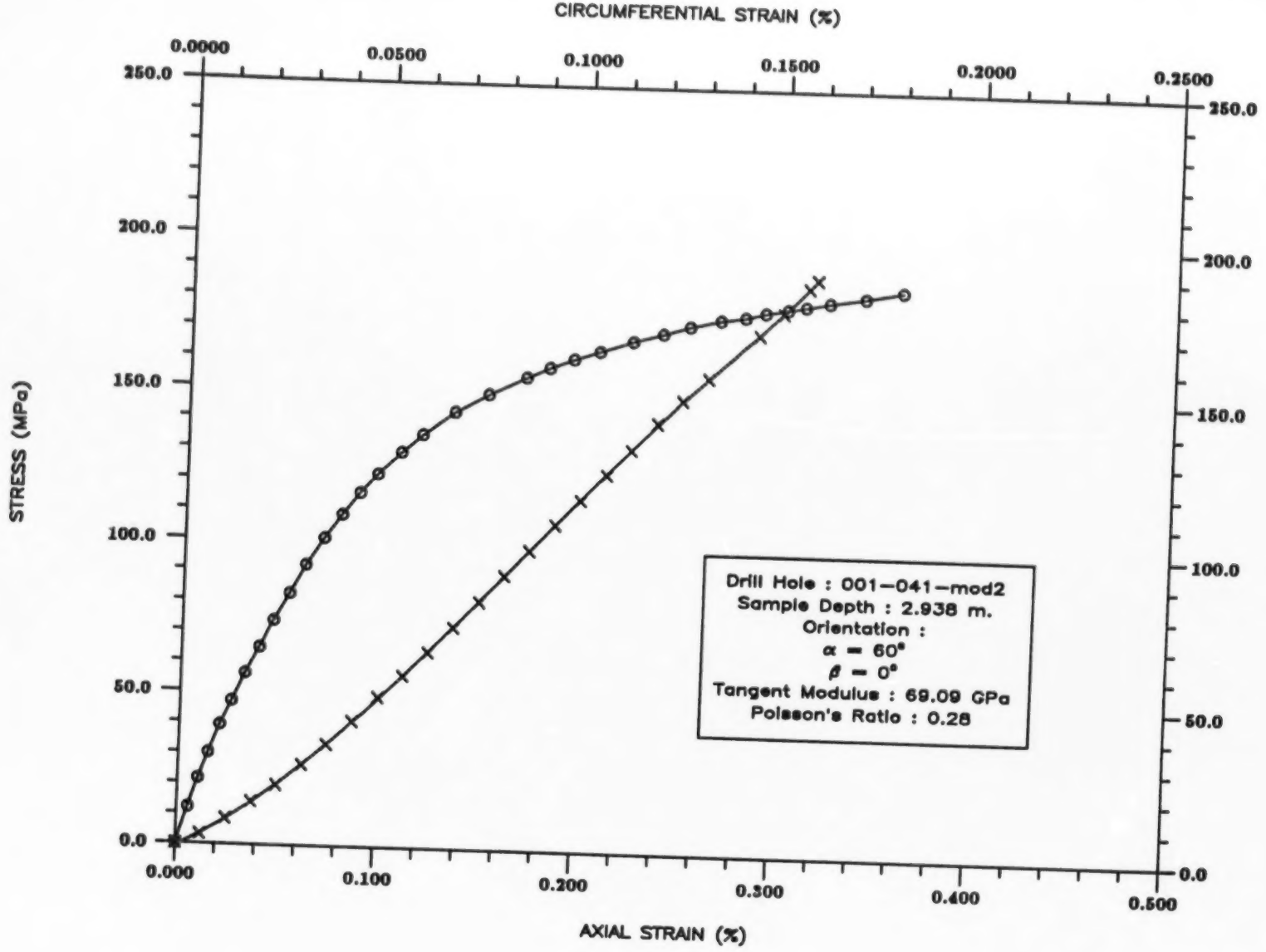

Fig. 31 : Axial and circumferential stress/strain curves for anisotropy test specimens.

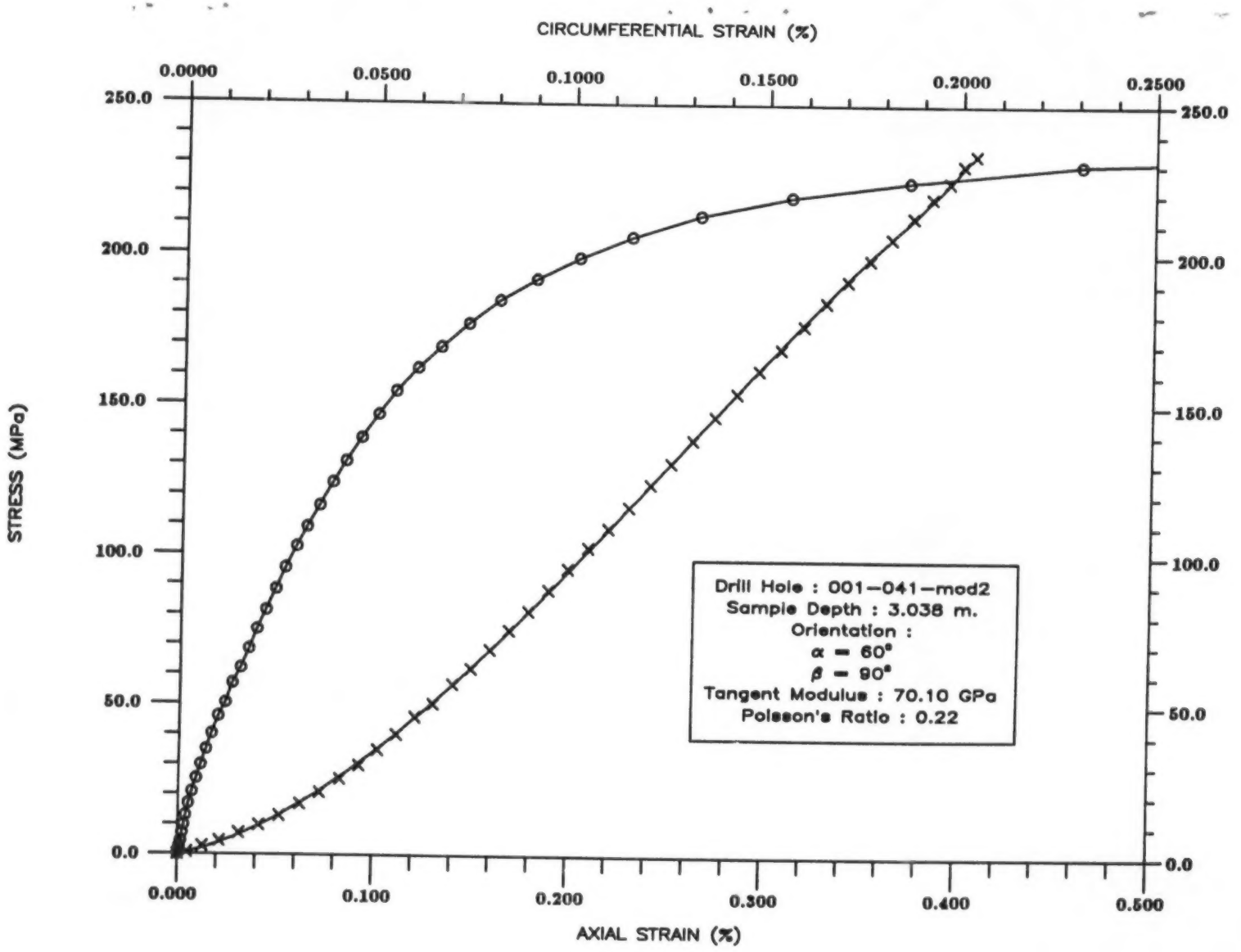

Fig. 32: Axial and circumferential stress/strain curves for anisotropy test specimens.

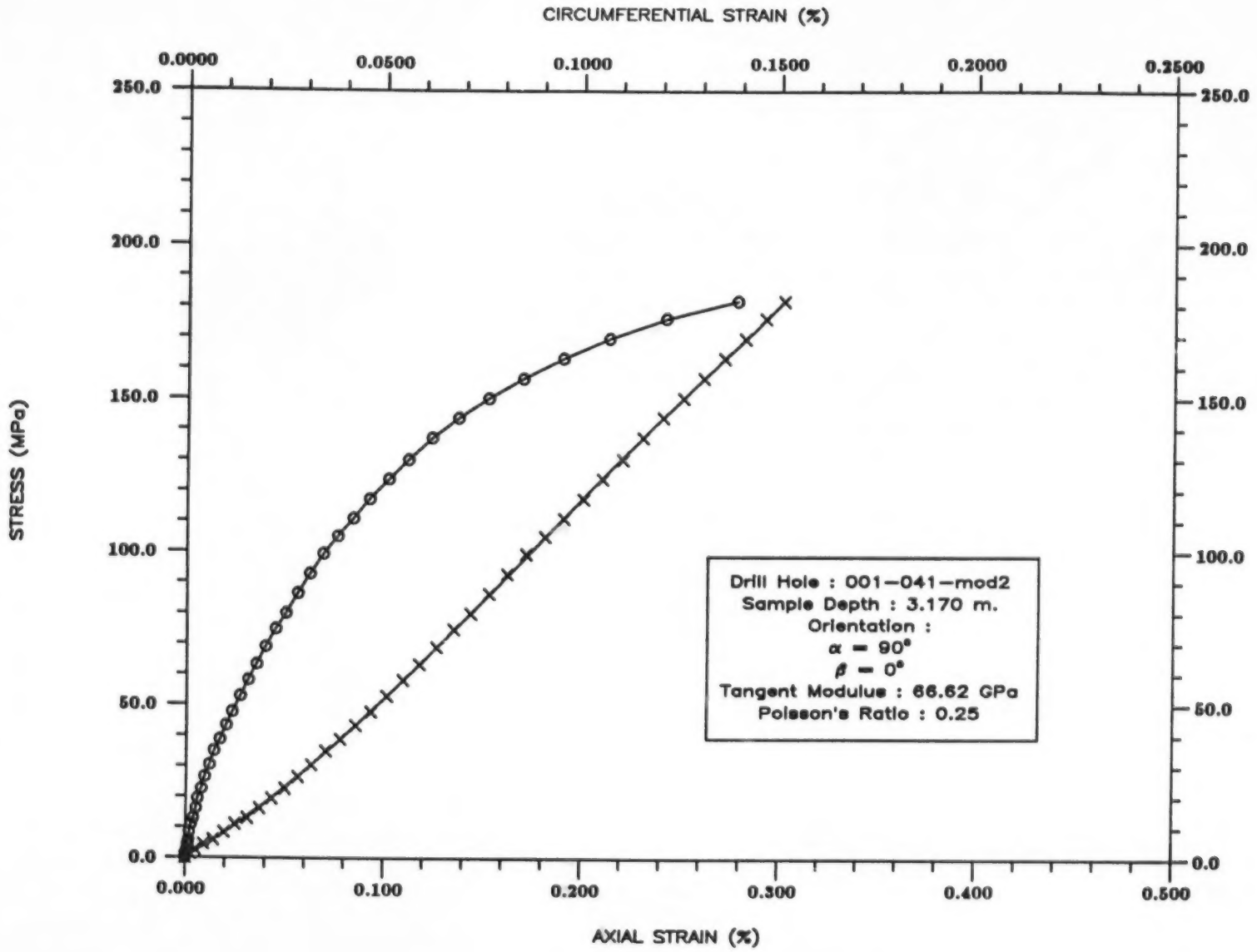

Fig. 33: Axial and circumferential stress/strain curves for anisotropy test specimens.

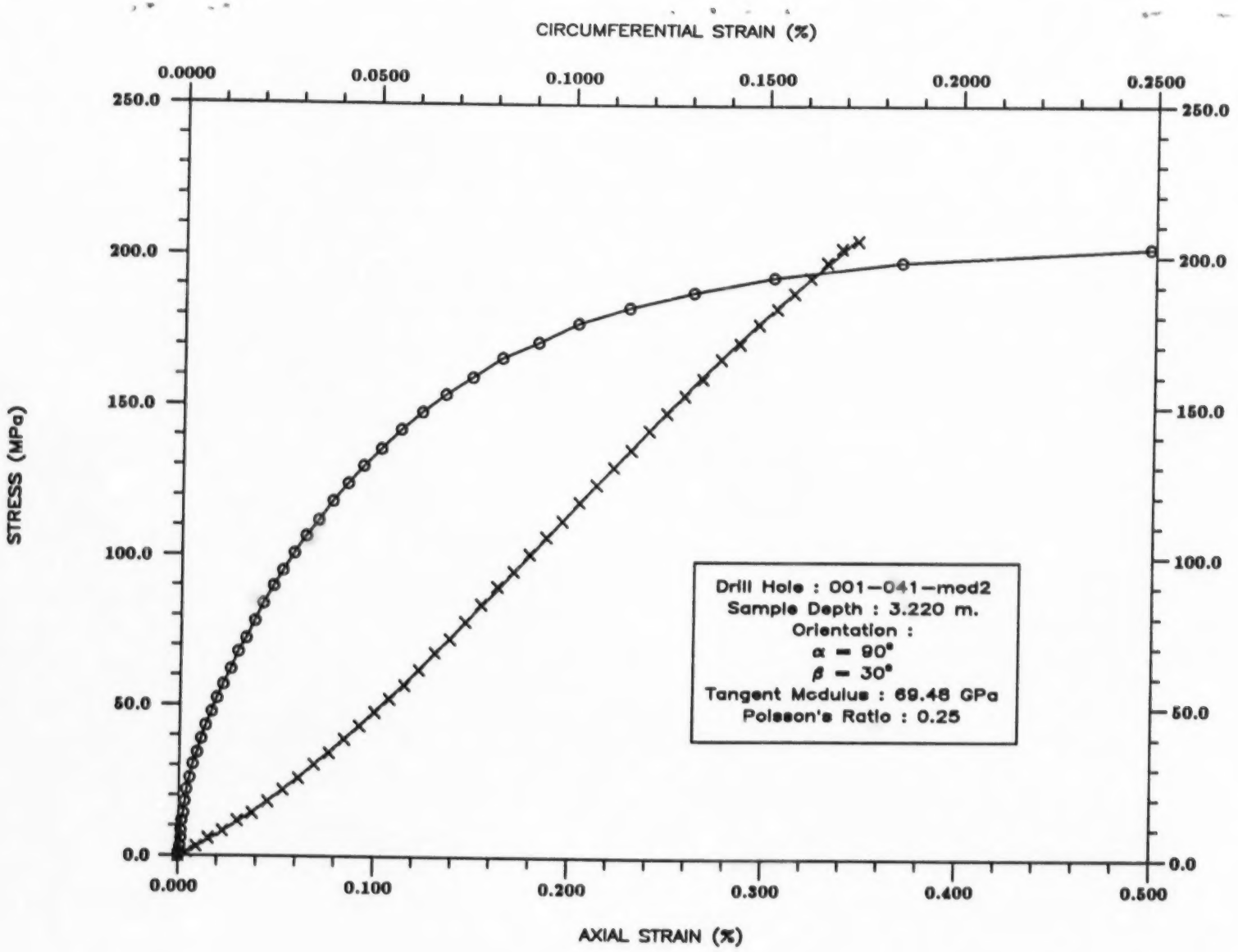

Fig. 34: Axial and circumferential stress/strain curves for anisotropy test specimens.

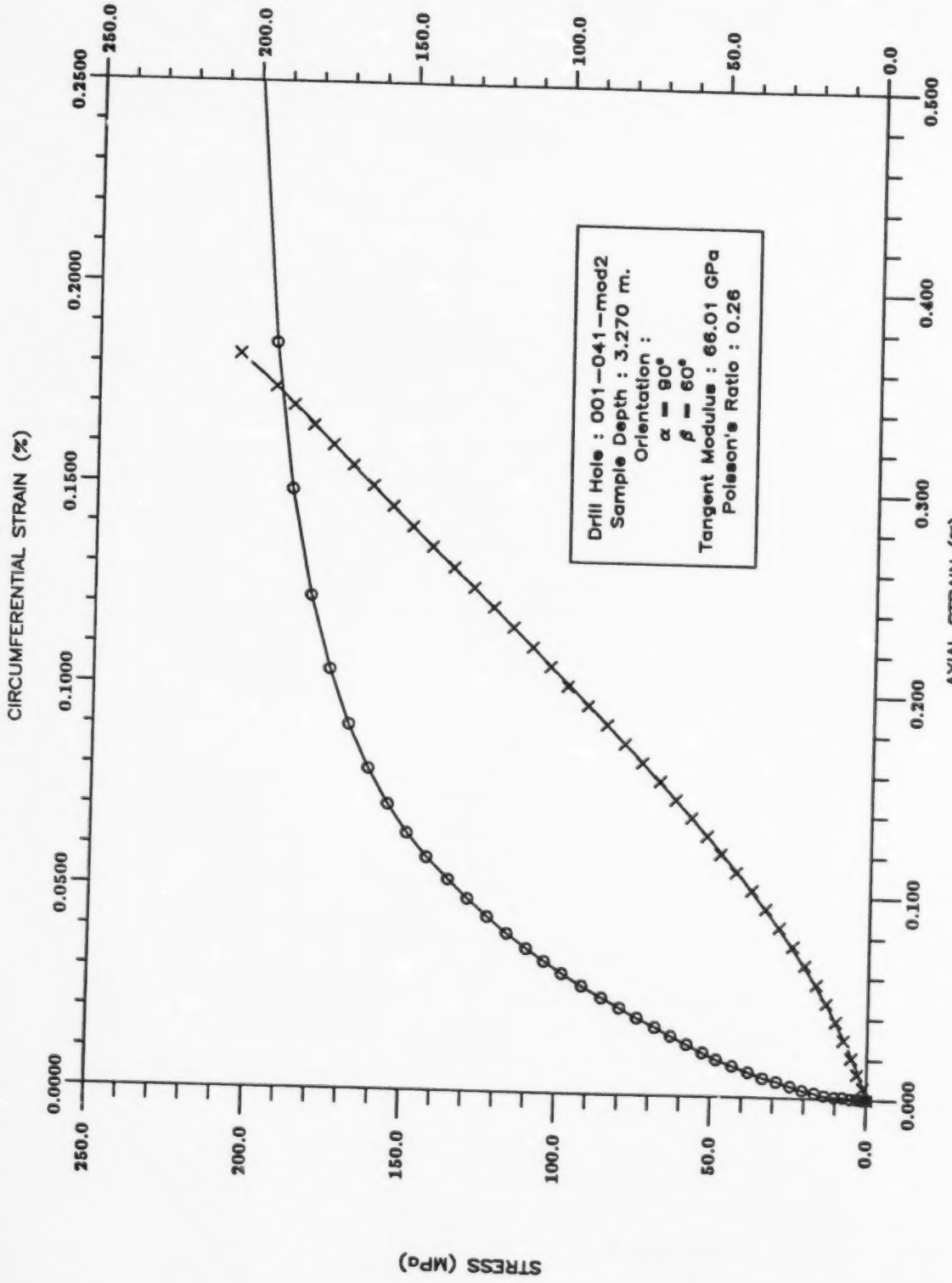

Fig. 35: Axial and circumferential stress/strain curves for anisotropy test specimens.

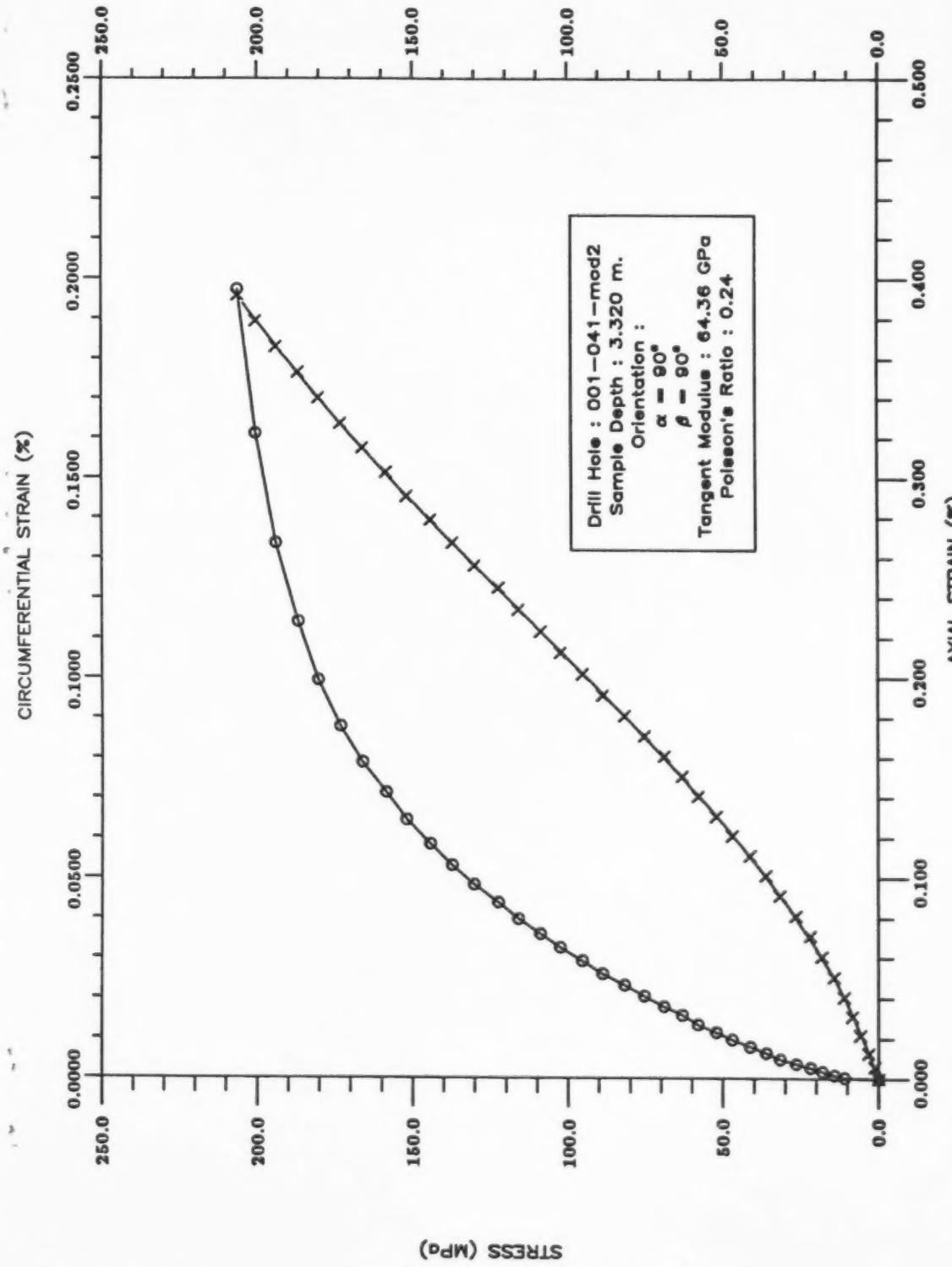

Fig. 36: Axial and circumferential stress/strain curves for anisotropy test specimens.